The Squeeze Film Damper over Four Decades of Investigations. Part II: Rotordynamic Analyses with Rigid and Flexible Rotors

G. Adiletta and L. Della Pietra

ABSTRACT—The present paper is aimed at summarizing the main results of the investigation regarding the application of the Squeeze Film Damper (SFD). Part I of the paper illustrated the constructive aspects and the operating features of this component, with reference to the related published work. Herein is a brief review of a number of theoretical and experimental analyses, regarding the dynamic behavior of rigid and flexible rotors supported with SFDs, with parallel examination of the main models adopted for the study. Advantages and drawbacks of SFDs are thus directly inferred from rotordynamic evaluation. Recent and current investigation, with particular regard to unconventional, improved SFDs, is briefly outlined in the concluding section of the paper.

KEYWORDS: Squeeze film damper, dynamics of rotors, damper bearings.

1. Introduction

In Part I of the present review [1] the Squeeze Film Damper (SFD) was examined as a separate component for turbomachinery, focusing upon its dynamic characteristics, through a short review of the main results inferred from a considerable series of theoretical and experimental investigations published since the 1960s.

The characterization of the damper, both in structural and operating terms, made it possible to gain a deeper insight into the dynamics of rotors equipped with this component. In fact, a significant part of the investigations in this area addressed the analysis of theoretical and experimental models of rotor-support systems. In this respect, a number of rotordynamic evaluations of the SF supporting were carried out, in close connection with the studies that were dealt with in [1]. A summary of the most outstanding results is given in the present paper.

As shown in the previous part [1], the adoption of the SFD for supporting either rigid or flexible rotors is mainly justified by the need to limit the effects of the residual unbalance, in terms of vibration amplitude and action transmitted to the frame through the rotor supports. These benefits can be achieved thanks to the presence of the lubricating film, with its nonlinear damping properties, to which a system of retaining springs is incidentally coupled. The latter are introduced in a number of arrangements, with the aim of centering the journals within the damper bearings, mounted parallel to the film, thus making the squeeze film and the elastic elements perform just like a suspension, with regard to the whole rotor-support system. An outstanding feature of the SFD supports is thus represented by a certain capability of tuning the system, in order to suitably position the operative range of speed relative to the zones affected by the occurrence of resonance phenomena.

Furthermore, some limitation of instability phenomena that can affect the dynamic response of turbomachinery under operating conditions, with the occurrence of nonsynchronous vibrations, can be attained thanks to the adoption of SFDs (see section 1 in [1]). Nevertheless, the nonlinear character of the fluid film forces of the SFD can introduce effects that nullify the expected benefits and go so far as to worsen the dynamic response of the rotor, as compared to the response obtained for conditions with rigid supports and absence of SFDs. Thus, the occurrence of *bistable* conditions, with typical *jump* phenomena, the unexpected amplification of the forces transmitted to the frame of the rotor and the rise of nonsynchronous motions, incompatible with *normal* operating conditions, are serious drawbacks arising from the incorrect design and use of SFDs.

As a matter of convenience, the following review was given a schematic approach. It reports a number of theoretical and experimental investigations, moving from the simplest *basic* models for rotordynamic analysis in the presence of SF supports, up to more complex, *extended* models that are somewhat closer to the real rotors for practical applications. A short survey of the most recent and current research reporting some examples of improved technical solutions is given in the end of the paper, thereby suggesting possible avenues for future investigation.

2. Basic Models for Analysis

Analysis of rotor motion, with attention paid to the effects of the main system parameters (rotor unbalance, geometrical parameters of the damper, characteristics of the fluid film, flexibility of the rotor and supports, etc.) in terms of amplitude, character and stability of the rotor whirl, and

Dipartimento di Ingegneria Meccanica per l'Energetica, Università degli Studi "Federico II", Napoli, Italy

The Shock and Vibration Digest, Vol. 34, No. 2, March 2002 97-126
©2002 Sage Publications

forces transmitted through the supports, is the distinguishing feature of most theoretical and experimental studies referred to below.

A number of simplifying hypotheses are distinctive of the basic models for the rotor-support system adopted for these investigations. For instance, the symmetry of the system and the approximate characterization of the behavior of the oil film in the damper, according to the analytical models from the lubrication theory, are generally assumed.

With reference to the simple arrangement with the rotor supported at both ends, the above-mentioned conditions of symmetry consist in assuming the rotor symmetrical with respect to its middle plane, with equal isotropic supports. Basic models are generally *lumped* ones. When the flexibility of the rotor is taken into account, the whole mass is concentrated in the middle section of the elastic shaft or, alternatively, part of the mass (the *bearing mass*) can be placed in correspondence or about the supports at the ends of the shaft. Elastic isotropy of the shaft is further assumed, along with neglecting the bow that is due to the gravity load and the misalignment of the shaft within the supports. With regard to the whirling motion of the rotor, the above conditions are consistent with the hypothesis of plane character and absence of conical components. As a consequence, for assigned shaft speed, two degrees of freedom (DOF) are required in the case of simple rigid or flexible rotors, and four DOF are to be adopted in order to study the dynamics of a symmetric flexible rotor with mass placed at mid-span and supports.

As regards the external active forces applied to the rotor, the analyses carried out with elementary models generally restrict the interest to the unbalance, assumed of static nature, and the gravity load.

The fluid film in the damper is characterized by means of approximate analytical models, with particular prominence given to the *short bearing approximation* (SBA), to the exclusion of the aspects related to the effects of lubricant inertia, supply (presence and type of holes and grooves for oil supply and drain) and seals. The length of the film is assumed to be 2π, when the pressurization makes the film uncavitated, or π. The latter assumption represents the usual way in order to readily treat cavitated conditions, especially for unpressurized conditions (supply pressure at the atmospheric value), regardless of the actual mechanism of film rupture (see [1] and section 3.5). Thus, analytical expressions for the fluid film reactions can be directly adopted in the equations of rotor motion.

A fairly straightforward analysis of the dynamic problem is possible provided that the hypothesis of synchronous circular centered orbits (SCCOs) of the damper journals in the respective bearings is assumed for the steady whirling motion of the rotor at a given speed.

It is worth noting that the hypothesis of circular centered orbits (CCOs) is consistent with that of isotropic supports. This last feature is certainly verified for the squeeze film, provided that the journals of the dampers are centered in the respective bearings for static conditions, i.e. when the rotor is *centralized* or *centrally preloaded*. Despite representing a condition realized in practice only more or less approximately, the initial centering of the journals by means of elastic elements further allows the equations of motions for the horizontal rotor to be expressed without the explicit presence of the weight and the preload of the retainer springs. In this manner, the axial-symmetry of the forces acting onto the rotor is assured. On the other hand, in the absence of retaining springs, the hypothesis of CCOs is congruent with the assumption of vertical axis of the rotor and absence of unidirectional radial loads (apart from the imbalance, the rotor is also said to be *unloaded*).

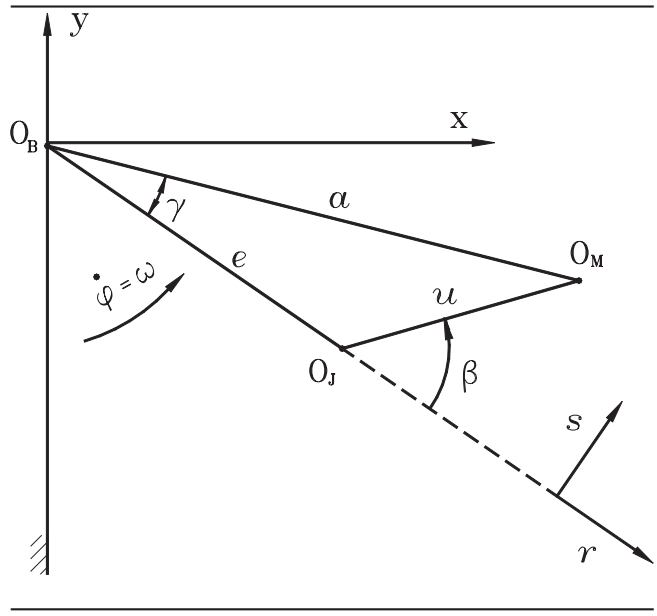

Figure 1. Relative positions of O_B, O_J, ed O_M for the rigid rotor, with synchronous, centered circular orbits of O_J

This is why the elementary models for rotordynamic evaluation of SFD performance assume centrally preloaded rotors or, alternatively, unloaded vertical rotors. It is worth noting that the previous axial symmetry of the forces is still acceptable in the presence of small static eccentricity of the journals, provided that the radius of the orbits covered by the same journals is small (see Section 3.2).

2.1. The Rigid Rotor

In the case of a rigid rotor at constant angular speed $\dot{\varphi} = \omega$, Figure 1 depicts the instantaneous position of the points O_B, O_J and O_M, that represent, respectively, the center of the damper bearing, the center of the damper journal and the mass center of the rotor. The figure also indicates the radius e of the journal orbit, frequently denoted as *journal eccentricity* (with respect to the bearing center), and the eccentricity u of the center of mass of the rotor with respect to the rotor axis.

Under the hypotheses that the orbits of the journal center are synchronous, centered and circular, the relative positions of the points O_B, O_J and O_M are constant with respect to time. With reference to the symbols adopted in the figure, assuming $2M$ the mass of the rotor, $2K$ the elastic rigidity of the centering springs, $-F_r$ and $-F_s$ the components of the damping film reaction along the coordinate directions r and s, respectively, the following relationships can be written for steady motion conditions:

$$M\left(e\omega^2 + u\omega^2 \cos\beta\right) - Ke - F_r = 0$$

$$Mu\omega^2 \sin\beta - F_s = 0. \quad (1)$$

The instantaneous position of the rotor is determined once the radius e of the circular orbit covered by O_J and the angular relative position β of O_M are obtained from the system (1). After giving approximate analytical expressions to F_r and F_s, as functions of e, thanks to the hypothesis of SCCOs of the journals, equations (1) represent a system of nonlinear algebraic equations. When $K = 0$, equations (1) represent the motion of a symmetric rotor with no elastic supporting elements, vertical axis and each point of the axis (represented by the journal center) covering circular centered orbits. In this circumstance, according to the first of equations (1), circular centered orbits can exist on condition that the radial component of the fluid film action is different from zero and is directed towards the bearing center O_B. Therefore, as long as the operating conditions make the film uncavitated and $F_r = 0$ [1], this equilibrium attitude is impossible unless $K \neq 0$ (for $K = 0$, from Figure 1 it can be inferred that the first equation is satisfied on condition that $\gamma = \pi / 2$, but the corresponding orbits are unstable; a demonstration of this result can be found, for instance, in [2]).

The stability of the steady solutions can be studied after linearization of the system about the steady equilibrium state, according to the general theory of stability (see for instance [3]), on the basis of the roots of the characteristic equation written for the local *perturbed* motion. Once the linearized dynamic coefficients of stiffness and damping are adopted, the regions of system stability can be determined with the *Routh–Hurwitz* criterion, regardless of the actual values of the characteristic roots. When the degree of damping is of interest, the roots are worth determining and numerical iterative procedures can be adopted.

Analysis of the dynamic behavior of the rotor-support system is generally carried out in dimensionless terms, with use of suitable parameters. The *unbalance parameter U* represents the ratio between the eccentricity u of the mass center of the rotor and the radial clearance C of the damper. A second dimensionless term, the *bearing parameter*, is connected to the damper characteristics and is expressed as:

$$B = \frac{\mu RL^3}{M\omega C^3} \text{ or } B_n = \frac{\mu RL^3}{M\omega_n C^3}. \quad (2)$$

In the above ratios, μ is the absolute viscosity of the lubricant. The geometry of the damper is represented by its radius R, the axial length L and the radial clearance C. The half mass M of rotor is multiplied by the angular speed ω of rotor or the *reference* natural frequency of the retainer spring-rotor system $\omega_n = \sqrt{K/M}$. Importantly, B_n can be adopted when $K \neq 0$ and the product $M\omega_n$ represents a sort of critical damping coefficient (except for the lack of a doubling factor).

A third dimensionless number, known as the *speed parameter*, is adopted for expressing the rotor angular speed ω. When $K \neq 0$, this parameter is generally represented by the ratio ω / ω_n. If the elastic suspension in the SFD is absent, the *reciprocal* of the bearing parameter B can be assumed.

The results of the analysis of the dynamic behavior of the rotor are generally expressed as *amplitude-frequency responses*, *phase diagrams* and *transmissibility diagrams*. These curves show, respectively, the dimensionless eccentricity $\varepsilon = e/C$ of the journal with respect to the bearing center, the angle β (Figure 1) and the dimensionless force $F / Mu\omega^2$ transmitted to the supports, as a function of the speed parameter, with assigned values of the bearing parameter and unbalance parameter. In particular, the ratio $T = F / Mu\omega^2$ is also indicated as *transmissibility* [1].

Investigations into the motion of the rigid rotor, according to Figure 1, were carried out under the πSBA (SBA, with π-film conditions) in [4–7], and both the πSBA and the 2πSBA (SBA, with 2π-film conditions) in [8, 9]. Both the SBA and the Warner approximation [1] were adopted in [2, 10]. In the course of these studies the effects of fluid inertia on the damper response were ignored.

In the absence of retaining springs ($K = 0$), as was previously observed, the hypothesis of centered orbits is congruent with the assumption of vertical axis of the rotor and absence of unidirectional radial loads. The frequency responses obtained from equations (1) with $K = 0$, for different values of the unbalance parameter U, have been depicted in Figure 2 as (ε, σ) plots, with $\sigma = 1/B = M\omega C^3/(\mu RL^3)$ representing the speed parameter. The fluid film force was expressed by means of the $\overline{C}_{ij}$ coefficients corresponding to the πSBA (Table 1 in [1]). From the figure, it can be inferred that, whatever the value of U, three solutions for the radius of the equilibrium orbits coexist above a threshold value of σ. In particular, the intermediate value of each term of ε solutions corresponds to unstable conditions [4].

Consequently, rotor operation may cause *jump* phenomena to arise. If $U < 0.44$, a *jump up* may occur with an increase in the operating speed: in this case the center of the journal jumps from an orbit whose radius is about the unbalance value ($\varepsilon \approx U$) to a larger orbit, whose amplitude tends to the clearance value ($\varepsilon \to 1$). By contrast, raising the angular speed in the presence of unbalances $U > 0.44$ may cause a *jump down* to take place, with an abrupt change in orbit radius to a smaller value (*inverted orbit*) that is about that of the static unbalance ($\varepsilon \to U$). From Figure 2 it can also be inferred that the farther U values are from 0.44, the higher the σ values that correspond to multiple solutions, i.e. the higher the ω values where jump phenomena can take place. Therefore when the unbalances are either quite small or high, the multiple solutions zone is above the rotor's operating range. In addition to Figure 2, the dynamic behavior of the unbalanced rotor is also illustrated by the plots (T, σ) and (β, σ) given in Figure 3(a),(b), respectively, and obtained from equations (1) under the same hypotheses.

Examples of analysis carried out with this model (unloaded vertical rotor and SFDs characterized with the πSBA), are represented by [2, 4]. White [4] numerically and graphically solved the algebraic equations of motions. Besides investigating the stability of the solutions, he carried out experimental tests that confirmed, albeit from a qualitative point of view, the existence of *bistable conditions* and jump phenomena. The jump up and jump down were observed through deceleration of the rotor, when values of unbalance higher and less than 0.55 were respectively adopted. This *separation* value proved different from the theoretically predicted 0.44.

With reference to the bistable conditions, White observed that, once given two co-existing stable orbits, the smaller one was ever characterized by a position of the center of

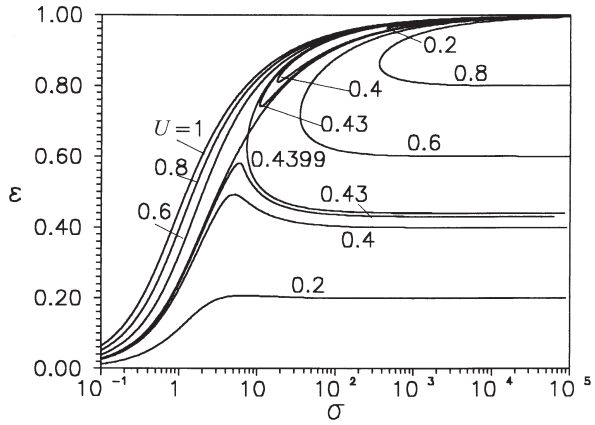

Figure 2. Theoretical frequency responses for the unbalanced rigid rotor (model according to Equations (1) with $K = 0$, different values of the unbalance parameter U, under the πSBA): dimensionless eccentricity ε vs. speed parameter σ

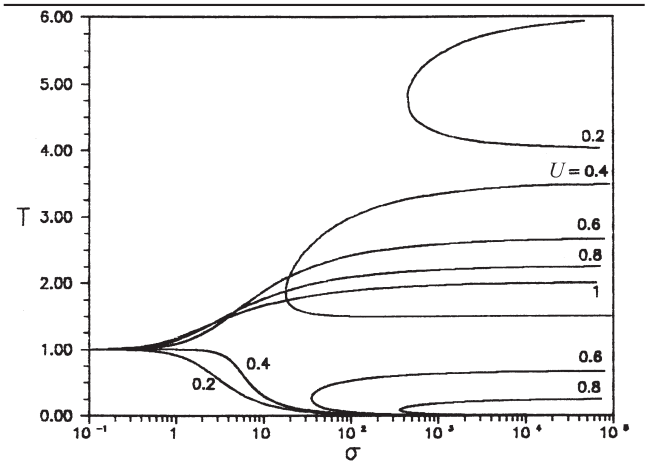

(a)

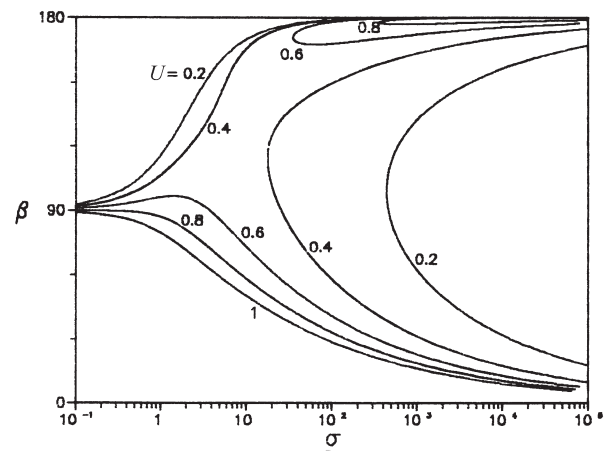

(b)

Figure 3. Theoretical frequency responses for the unbalanced rigid rotor (model according to equations (1) with $K = 0$, different values of the unbalance parameter U, under the πSBA): (a) transmissibility T vs. speed parameter σ; (b) angle β vs. speed parameter σ

mass that was internal with respect to the position of the journal center (*inverted orbit*).

Hahn [2] carried out a theoretical investigation (applicable to both the case of rotor on SFD supports and that with journal bearings) whose results were similar to those of White. The transmissibility plots in the paper amply prove that operation with T 1 is possible provided that U 0.43 and the jump up is avoided. Further data were obtained with use of the Warner approximation (WA) in place of the SBA and were applicable to dampers with L/D 0.5. In this case, the journal eccentricity responses and the transmissibility diagrams were dependent (among the other parameters) on the actual value of the L/D ratio, but turned out to be qualitatively similar to the corresponding ones obtained for the short bearing model (L/D 0.5). In particular, in order to guarantee T 1 (in the absence of jump up, whatever the L/D value), an upper limit of 0.61 was predicted with the WA for the unbalance parameter, in place of that of 0.43 obtained with the SBA.

When the rotor is provided with centering springs it is somewhat difficult to plot diagrams that have a general validity, such as those depicted in Figures 2 and 3, since the dynamic behavior depends further on the stiffness of the elastic suspension.

Some general diagrams for design purpose were given in compact form [5, 6] and showed that the dynamic behavior of an elastically centered rotor is similar to that of the unconstrained rotor with vertical axis. The tendency of the orbit radius ε towards the unbalance value, when $T < 1$ and SFD operates with its highest degree of efficiency, and the possibility of bistable operation were apparent from the given results. As in the case of an unconstrained rotor with vertical axis, the intermediate solution of each tern representing co-existing solutions was unstable [2, 9].

Mohan and Hahn [6] carried out a parametric characterization of the horizontal centralized rotor (with the πSBA) from a design standpoint. In the expression of the bearing parameter, the design speed of the rotor was adopted in place of the natural frequency ω_n (or the actual speed ω) and the ratio between ω_n and the design speed was introduced as a *spring parameter*. The *critical unbalance*, i.e. the "maximum unbalance that can be tolerated before the squeeze film bearing mount is worse than a rigid support", was evaluated by varying the bearing and spring parameters. The *transmissibility at design speed* was also plotted as a function of the bearing parameter, for different values of the unbalance and spring parameters. The influence of the different parameters on the *transmissibility at resonance* was further evaluated. These data illustrated the existence of a wide range of parameters that were capable of assuring small values of the forces transmitted through supports during operation. The need to assign the lowest possible stiffness of the retainer springs was also inferred (provided that the centering of the journals is assured). The same data showed that the choice of the bearing parameter deserved some care, since neither too high nor too low values were advisable. In the first case, an increase in the transmissibility at design speed was to be expected, while a rise in the transmissibility at resonance derived in the latter case.

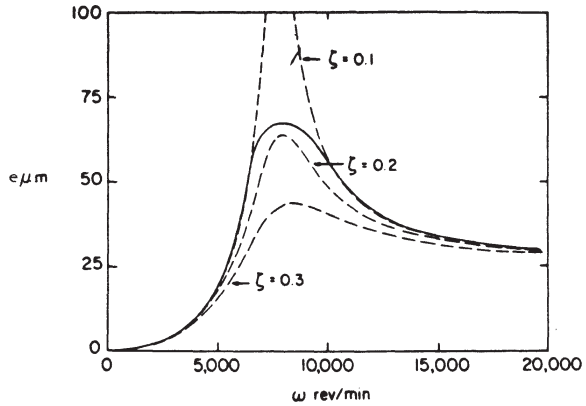

Figure 4. Theoretical frequency responses for the unbalanced rigid rotor with centering springs and assigned values of the parameters, under 2π-film conditions: the eccentricity *e* vs. shaft speed ω plot (solid curve) is compared to the responses from a linear model (dashed curves) with the same unbalance, spring stiffness and different damping ratios ζ (reproduced by permission of the ASME [9])

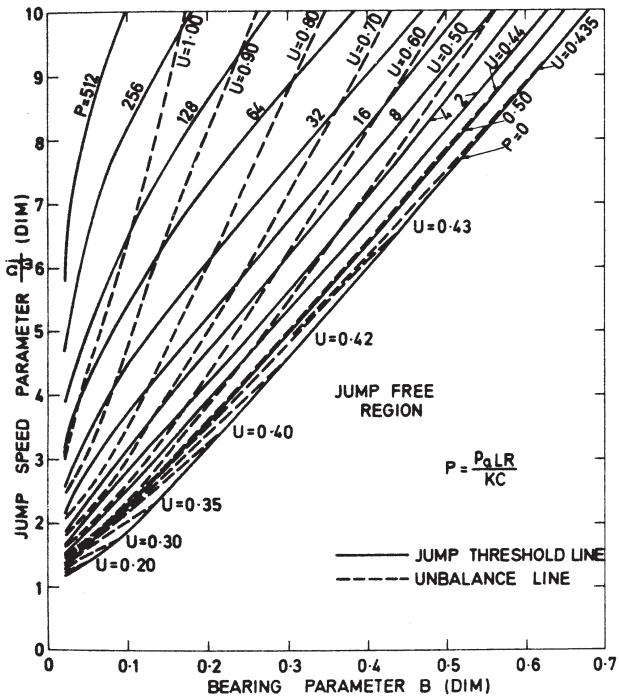

Figure 5. Dependence of the jump speed on the supply pressure (represented by the dimensionless ratio $P = p_aLR/(KC)$, the bearing parameter and the unbalance parameter (reproduced by permission of the ASME [11])

The above data were also reported in [5], with slight differences in the use and expression of parameters (the bearing parameter was represented by the ratio B_n of (2) and the speed parameter ω / ω_n was adopted for characterization in place of the spring parameter). The dependence of the critical unbalance ("the unbalance at which the transmissibility exceeds one, or at which the uninverted operation mode is possible") on the various parameters was more clearly illustrated and the associated possibility of jump was highlighted.

When the film is uncavitated (2π-film) the response of the unbalanced rotor proves quite different from the case with cavitation. If the SBA is adopted it can be shown that multistable operation is impossible. It must be also stressed that the presence of radial stiffness represents a necessary and sufficient condition for the stability of the centered orbits. By contrast, when $L/D \geq 0.5$, analysis with the WA allows us to maintain that the stability can be assured even in the absence of radial stiffness, depending on the L/D value. An illustration of these results can be found in [2].

Figure 4, from [9], illustrates the theoretical frequency response for an elastically centered rotor with the SFDs operating under 2π-film conditions. The nonlinear rotor response was compared with those obtained from a linear model with the same unbalance and spring stiffness, for different values of the damping ratio.

Simandiri and Hahn [11] studied the influence of the size of the pressurized arc within the film. Careful characterization of the bistable behavior and occurrence of jump (up and down) was reported in their paper. The authors determined the effective length of the film as a function of the supply pressure (the damper was treated in accordance with to the SBA, with atmospheric pressure at the discharge-end and an arbitrary value of the supply pressure p_a at the opposite end) and the value of the pressure in the cavitated zone (i.e. the *saturated vapor pressure* that was assumed atmospheric). The film reaction was thus evaluated according to the determined film conditions. On this basis, the unpressurized damper-case was studied along with those cases characterized by non-null *supply pressure parameter* (expressed by means of the ratio $p_aLR/(KC)$, which was given values up to 512 in the course of the analysis). The dependence of the jump (up and down) speeds on the supply pressure, unbalance parameter and bearing parameter was illustrated in a series of maps (Figure 5). A second series of diagrams illustrated the influence of the same parameters on the orbit eccentricity and the transmissibility *T*. These results show the broadening of the *jump free region*, i.e. the operating range corresponding to the absence of multiple solutions and jumps, as a consequence of raising the supply pressure level. If the supply pressure was sufficient to achieve an uncavitated film, the radial component of the fluid force was nullified and the possibility of bistable operation vanished. The consequent reduction in the orbit amplitudes was also evident. However, at the same time, the increase in pressure made *T* increase. The diagrams showed that the same effect, in the jump free region, was obtained by increasing the bearing parameter. It was also recognized that the beneficial effect of raising the unbalance, as a means of countering the bistable behavior, is only apparent because of the consequent unacceptable increase in the transmissibility.

In line with these investigations, the studies [8, 10] are to be considered. However, in these papers the model was generalized to some extent and the related results have hence been reported below, in section 3.2.

Instead of solving the algebraic equations like those represented by equations (1), the theoretical investigation of Taylor and Kumar [9] was carried out with direct numerical integration of the differential equations of motions (see section 3.1). The influence of the initial conditions was

analyzed for both 2π and π-film conditions. In particular, under the latter conditions, in the interval of speeds with bistable behavior, i.e. in the presence of two co-existing stable solutions, the authors observed that a more extensive region of initial conditions from which the solutions converged was corresponding to the smaller orbit. This result was explained as an effect of the dominant character of the solutions on the lower branch of the *amplitude-frequency* diagram. Recourse to the numerical integration of the equations of motion, written for the rigid rotor, was shared by other investigations, which will be referred to below in section 3.1.

2.2. The Simple Flexible Rotor

Two models for the simple flexible rotor, supported with identical SFDs at both ends of the elastic shaft, are depicted in Figures 6(a) and (b) (from [12, 13], respectively).

A mathematical model for this case can be written with reference to Figure 7. The plane of the figure coincides with the mid-span plane of the rotor. According to the symmetry of the rotor with respect to its middle plane, only one half of the rotor can be assumed for the model and represented by means of projection onto the plane of the figure. Points O_B and O_J represent the center of the bearing and that of the journal, respectively. Point O_R, distant p from O_J, represents the trace of the rotor axis in the middle plane and the segment $\overline{O_J O_R}$ represents the shaft deflection. The whole mass of the rotor can be concentrated in its center, in the middle plane of the rotor or, alternatively, placed partly in the same plane and partly at the supports. Hence, with reference to Figure 7, the half mass of the rotor is assumed to be concentrated in the center of mass O_M or divided between O_M and O_J. The relative position of O_M with respect to O_R is given by the eccentricity u and the angle β. In the model, the static deflection of the rotor shaft is neglected. In the figure, the angular speed of the rotor is assumed to be represented by the angular speed of the segment $O_R O_M$ with respect to the frame of reference. The motion of precession (or whirling) of the rotor can be represented by the trajectory of the rotor center O_R or that of the journal center O_J, with $\dot{\varphi}$ representing its angular frequency. With reference to the notation in Figure 7, the equations of motion are (for instance [14]):

$$\begin{cases} -\alpha M(\ddot{e} - e\dot{\varphi}^2) + k_s p\cos\phi - k_r e - F_r = 0 \\ -\alpha M(e\ddot{\varphi} + 2\dot{e}\dot{\varphi}) + k_s p\sin\phi - F_s = 0 \\ -(1-\alpha)M[\ddot{q} - q(\dot{\varphi}+\dot{\xi})^2 - u\omega^2\cos\beta] \\ \quad - k_s p\cos(\phi - \xi) - \zeta\dot{q} = 0 \\ -(1-\alpha)M[q(\ddot{\varphi}+\ddot{\xi}) + 2\dot{q}(\dot{\varphi}+\dot{\xi}) - u\omega^2\sin\beta] \\ \quad - k_s p\sin(\phi - \xi) - \zeta q(\dot{\varphi}+\dot{\xi}) = 0. \end{cases} \tag{3}$$

The stiffness coefficients k_s and k_r are relative to the half shaft and the retainer springs of the SFD, respectively. The viscous damping in the middle plane of the rotor is represented by the coefficient ζ. The α *mass ratio* between the mass at support placed in O_J and the whole mass M of the half rotor represents a parameter of the system. As regards the other parameters in the analysis, shaft flexibility makes it possible to express the bearing parameter and speed

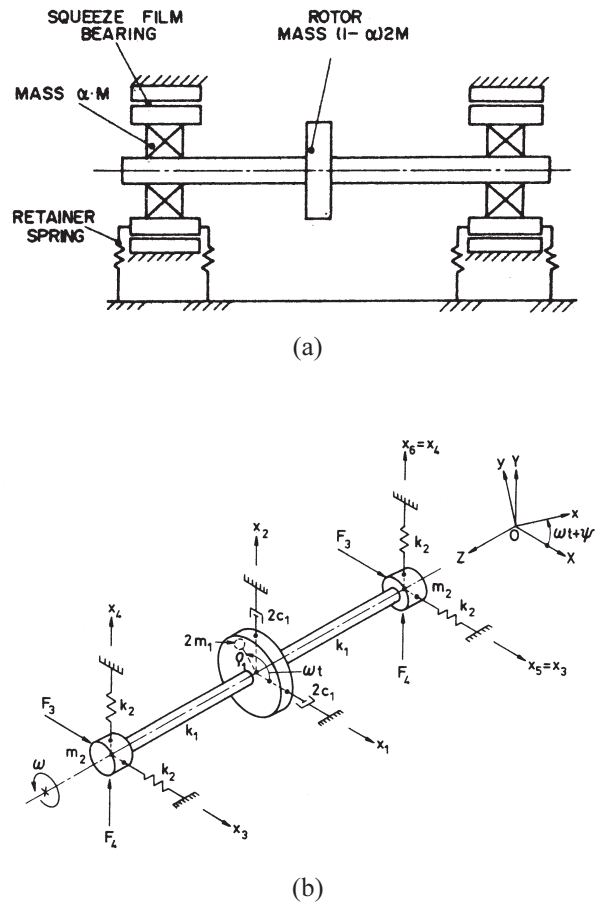

Figure 6. Theoretical models for the analysis of flexible rotor: (a) reproduced by permission of the ASME [12]; (b) reproduced by permission of the ASME [13]

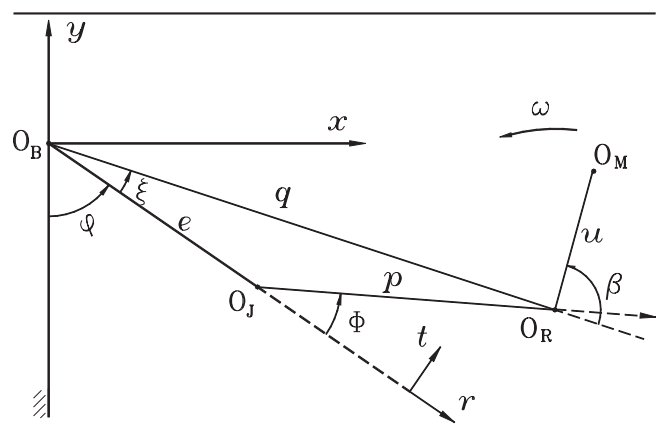

Figure 7. Relative positions of O_B, O_J, O_R and O_M for the flexible rotor

parameter as a function of the *first pin-pin critical speed* ω_c (i.e. the natural frequency of the first flexural mode of the rotor on rigid supports), especially when, in the absence of centering springs, $\omega_n = 0$. An additional parameter, known sometimes as the *resonance frequency ratio*, expresses the ratio f between ω_n and ω_c. Both f and α are normally less

than one. Under the hypotheses of constant rotor speed ω and SCCOs of the journals of the SFDs, the time derivatives of e, q and ξ are null, $\dot{\varphi} = \omega$, $\ddot{\varphi} = 0$ and the differential equations (3) can be replaced by a system of algebraic equations.

The dynamic behavior of the flexible rotor, with SCCOs of the damper journal, was studied by White [4], Rabinowitz and Hahn [12, 14] and Cunningham et al. [15], who carried out a relatively complete analysis, and McLean and Hahn [13, 16], Hahn and Chen [17], Zhao et al. [18], who reported this case as an illustration of procedures for analyzing more complex rotors (see Section 3.4).

In these investigations, as in the studies referred to in the previous section, the damping film was mainly characterized with the πSBA. The stability of the synchronous steady state solutions of equations (3) can be analyzed with the approach indicated in the previous section. An example of application of the Routh–Hurwitz criterion was given in [12]. Examples of determination of the roots were reported in [4], where the Newton–Raphson procedure was adopted (along with the Routh–Hurwitz criterion), and in [13], where the numerical finding of the characteristic roots was carried out within an eigenvalue-problem approach.

A model of a flexible rotor, with masses at mid-span and supports, and SFDs equipped with centering suspensions, was theoretically investigated in [15]. Analysis was carried out in order to optimize the design of a real five masses-rotor, operating in a speed range beyond the second bending critical speed. A linear vibrating model with two degrees of freedom, in the presence of damping (see [19]), was adopted for selecting the dynamic characteristics of the SFDs. In particular, the authors first evaluated the stiffness and damping degree of the supports, in order to optimize the dynamic response, in terms of vibration amplitude and transmissibility. The geometry of the SFDs was then obtained after assigning the rotor unbalance and the maximum eccentricity of the journals ($\varepsilon = 0.4$), with use of the expression for the fluid film reaction (in this paper, as in [20–22], the film force was expressed by means of stiffness and damping coefficients) valid for CCOs.

In [14] the dynamic behavior of the rotor was studied after writing the system of algebraic equations obtained from (3) under the hypothesis of SCCOs, in the range of speed up to 3–5 times the value of the pin-pin critical speed, beyond the second bending critical speed. The SBA with π and 2π film lengths of the film was assumed in order to represent, respectively, cavitated conditions, in the absence of pressurization, or full film conditions, attained with a suitable level of the supply pressure. An example of the results reported in the paper is depicted in Figure 8(a), as a set of curves in the coordinate plane of the *rotor amplitude ratio* vs. the speed parameter (the *rotor amplitude ratio* was the nondimensional rotor amplitude of vibration G at mid-span divided by the unbalance parameter U; here $U = (1-\alpha)u/C$ and is indicated in the figure as U). The curves were obtained, for unpressurized conditions, with fixed values of the resonance frequency ratio f and the mass ratio α. Different sets of values of the bearing parameter B_n (indicated in the figure as B) and the unbalance parameter were adopted. Low damping at supports makes the rotor response dominated by the rigid mode, with resonance peaks near ω_n (values of the speed parameter a close to that of f). By

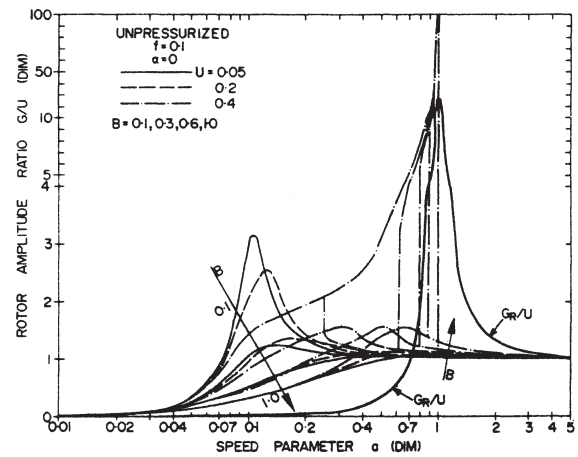

(a)

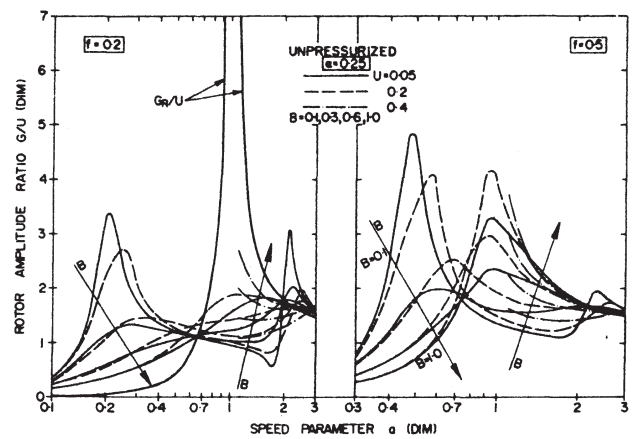

(b)

Figure 8. Amplitude-frequency curves for the centralized flexible rotor with different values of the operating parameters and unpressurized conditions: (a) $\alpha = 0$, $f = 0.1$; (b) $\alpha = 0.25$, $f = 0.2$ and 0.5 (reproduced by permission of the ASME [14])

contrast, the higher the B_n, the closer the peaks of resonance are to ω_c (a values close to 1). The shift towards the pin-pin critical speed indicates that the increase in the damping action of the SFDs emphasizes the influence of the rotor flexibility. The results also show the nonlinear sensitivity of the SFDs, being manifested in an attenuation of the resonance peaks that increases with the level of unbalance. The example in Figure 8(b) still refers to unpressurized conditions and is relative to different values of the parameters α and f. The existence of bistable conditions, in proximity of the pin-pin critical speed ω_c (i.e. when the $a \approx 1$), was also evident in these data. The higher the unbalance parameter and the lower the degree of damping, represented by the bearing parameter, the more likely was the existence of a range of speed with bistable operation (when U was given the highest value, equal to 0.4, the bistable behavior could occur whatever the value of the bearing parameter; it is worth pointing out that in Figure 8(b), the relative curves were omitted in the vicinity of $a = 1$). The results relative

to 2π-film conditions showed the effectiveness of pressurization as a means of avoiding bistable behavior, as was seen for the rigid rotor case. From the whole data relative to both π-film and 2π-film lengths, some indications could be further inferred. The observed rise in the amplitude of peaks at resonance with the mass ratio made the authors note the need to reduce the mass at supports, as guidelines for the design stage. A similar influence was played by the resonance frequency ratio, since the higher this ratio, the higher the maximum amplitude of the response. The same maximum amplitude appeared to be faintly affected by the film length adopted in the model. The transmissibility (in particular evaluated in a range of speed beyond the pin-pin critical speed) increased with the levels of damping at supports and rotor unbalance. A limitation of the transmitted forces, with respect to the case with rigid supports, could be assessed on the basis of the same data.

Interestingly, from a stability analysis of the above results [12], in the presence of multiple solutions, besides the solutions along the middle branch, as was seen for the rigid rotor case, instability could also affect the response at higher eccentricities. The same study showed that favourable conditions for the instability were characterized by high unbalances, low values of the bearing parameter – as in the case of rigid rotor – and, further, by high values of the mass ratio and small values of the resonance frequency ratio. Thus assigning the last two parameters, the authors obtained unstable solutions even in the presence of moderate unbalance ($U = 0.2$) and relatively high damping ($B_n = 0.6$). Yet, the analysis well characterized the zones internal to the operating range where the steady synchronous motion of the rotor was stable. The above results referred to π-film conditions. By contrast, the data obtained for the full film approximation (i.e. for pressurization conditions) showed the absence of instability whatever the fixed set of parameters. Hence, as for the rigid rotor, the usefulness of pressurization was confirmed in order to eliminate jump phenomena and give stability to the system, at least in such intervals of speed like that in question, and placed below the second flexural critical speed.

White [4] characterized the dynamic behavior of a flexible rotor with vertical axis, the whole mass being placed at mid-span (i.e. $\alpha = 0$) and SFDs mounted without centering springs. The theoretical diagrams of the journal eccentricity as a function of rotor unbalance, evaluated at fixed values of the speed parameter and bearing parameter (the latter represented by $1/B = M\omega C^3/(\mu RL^3)$), showed results that were substantially in agreement with those obtained in [14], for operating conditions that were approximately comparable, despite the differences in the respective models. In particular, the onset of bistable behavior was possible in the speed interval up to ω_c, as long as the rotor unbalance was not too low (U above $0.1 \div 0.2$) and B values were fixed in the range $0.2 \div 0.3$. In such circumstances, the existence of a threshold value for U, below which jump phenomena vanished, could be inferred for a given value of the bearing parameter: the lower the value of B, the lower the threshold value. In the presence of multiple solutions, White showed the instability of the journal orbits with intermediate values of the radius. Furthermore, unlike the rigid rotor case, as evidenced in [12], some instability was also found to affect the orbits with the higher radius value. In this regard White

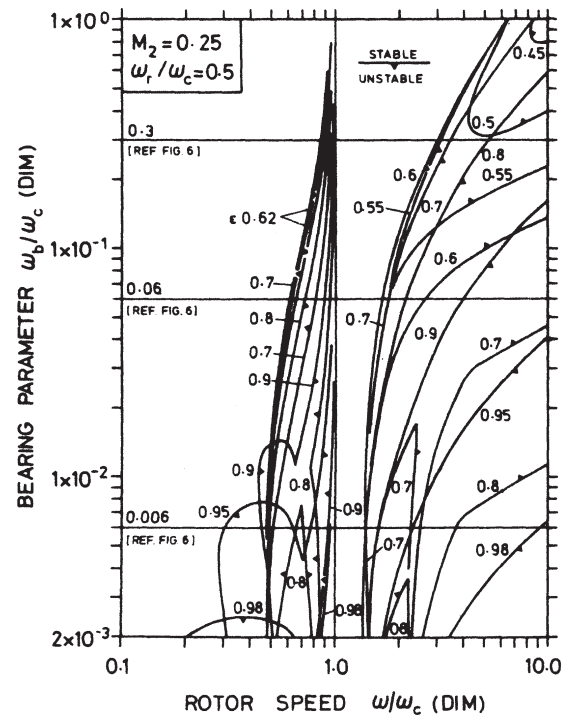

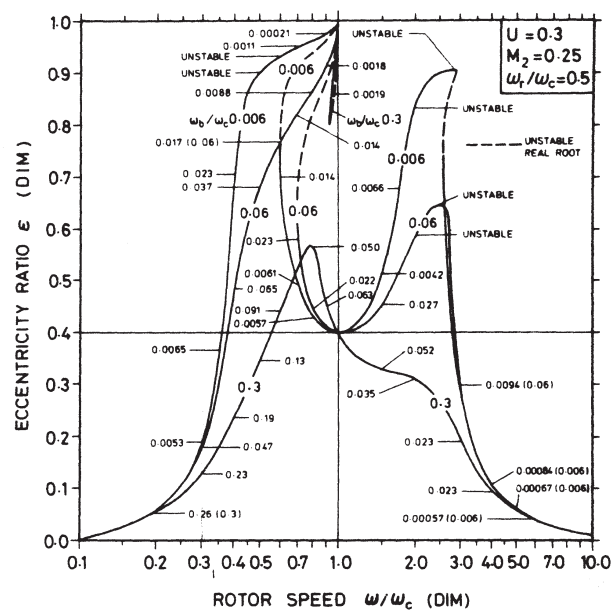

Figure 9. Stability analysis for the centralized flexible rotor, with fixed values of the mass parameter (M_2) and the frequency ratio (ω_r / ω_c), under π-film conditions: (a) instability map in the bearing parameter vs. speed parameter plane, for different radius ε of the SCCOs; (b) frequency responses for assigned unbalance parameter U and different values of the bearing parameter (ω_b / ω_c), with indication of the smallest damping ratio along the curves (reproduced by permission of the ASME [13])

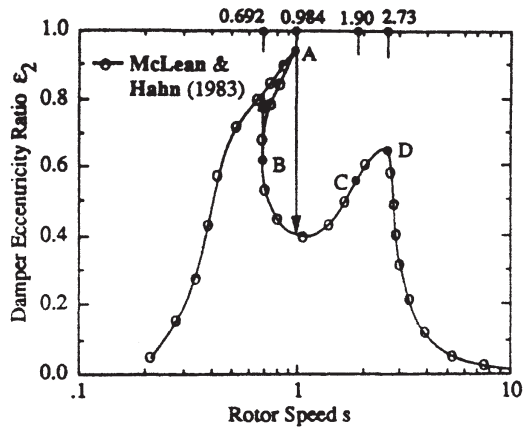

(a)

Figure 10(a). Theoretical analysis for the centralized flexible rotor (the values of the parameters were those of Figure 9b, with the bearing parameter equal to 0.06): (a) radius of the journal orbit vs rotor speed

noted the *near-neutral* stability that characterizes the solutions at higher eccentricities, with near-zero real part of the characteristic roots, so as to make the numerical analysis of stability difficult.

In [13, 16], the study of the centralized flexible rotor, in agreement with the model depicted in Figure 6(b), carried out under the hypothesis of SCCOs, was reported in order to illustrate a procedure for analyzing more complex rotors (see section 3.4). The authors obtained in a relatively straightforward way the amplitude-frequency responses corresponding to a fixed value of the unbalance parameter (U = 0.3) and three distinct values of the bearing parameter, respectively. Then, an instability map was plotted (Figure 9(a)) in the plane of parameters B_n, ω/ω_c, (B_n is represented in the figure by the ratio ω_b/ω_c) at constant values of the journal eccentricity ε (the *frequency ratio* ω_n/ω_c and the mass ratio α, indicated in Figure 9(a) and (b) respectively as ω_r/ω_c and M_2, were fixed as in [14] in order to allow comparability of results). A complementary representation of the results was partially given in the (more usual) plane of the parameters ε, ω/ω_c (Figure 9(b)). The data showed that, in the ranges of speed characterized by multiple solutions, the instability of the synchronous centered steady motion may affect not only the orbits with intermediate value of the radius, but also those with higher radius, though in some restricted intervals of speed. Narrow ranges with unstable character of the CCOs solution were also found outside the zones with multiple solution, when the bearing parameter was given the lowest of the three numerical values selected for the analysis. In other terms, the analysis predicted the existence of limited zones of operation with complete instability of the synchronous centered steady motion. On the other hand, under stable motion conditions, the authors calculated the smallest damping ratio $-\mathrm{Re}(\lambda)/|\mathrm{Im}(\lambda)|$, with λ representing a root of the characteristic equation, as a means of evaluating the degree of stability (Figure 9(b)).

The same example was subsequently adopted in [17] in order to illustrate an iterative procedure based on the harmonic balance method (HBM) and the Newton–Raphson method, more generally addressing nonlinear analysis for

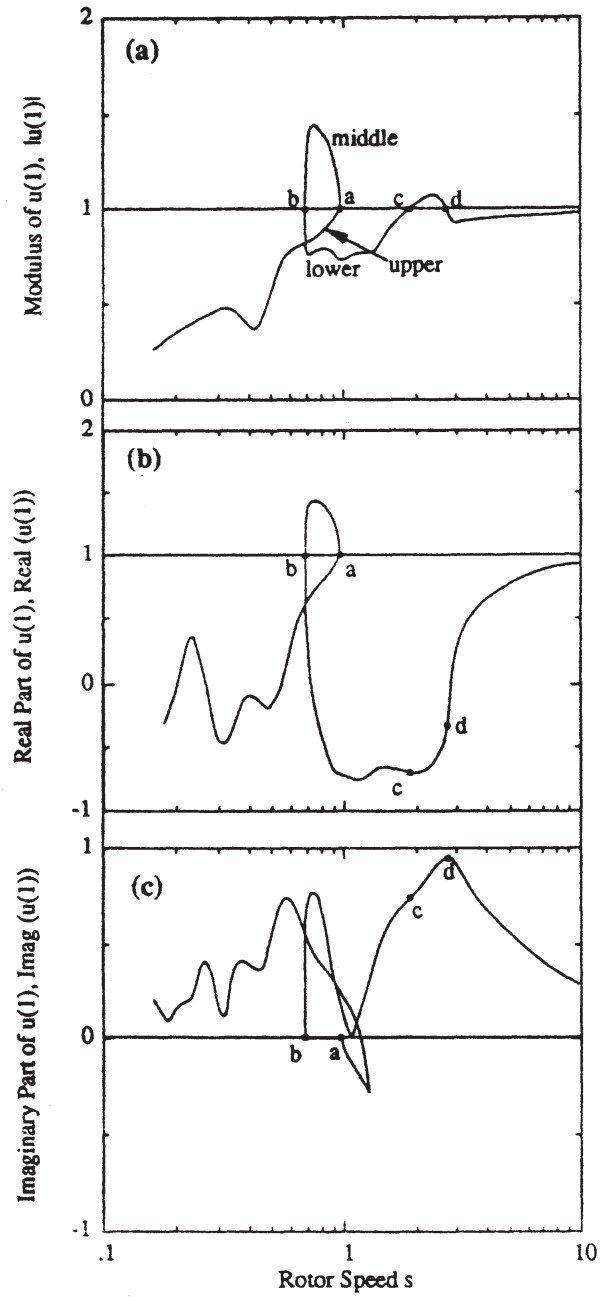

(b)

Figure 10(b). Theoretical analysis for the centralized flexible rotor (the values of the parameters were those of Fig. 9b, with the bearing parameter equal to 0.06): (b) modulus (top), real part (middle), and imaginary part (bottom) of the first Floquet multiplier vs rotor speed; points a, b, c, and d correspond to points A, B, C, and D in Figure 10a (reproduced by permission of the ASME [18])

real rotors (see section 3.4). The results agreed closely with those obtained from previous studies [12–14, 16] (some drawbacks of the procedure were observed when finding unstable solutions at intermediate eccentricity, in the regions with multiple solutions). Stability analysis was tackled with recourse to the Floquet method – though unnecessary in accordance with the simplifying hypothesis of SCCOs –

and confirmed the results reported in [13]. In particular, the unstable character of motion at high eccentricity was observed in some intervals of speed in the presence of the lowest values of the bearing parameter.

Zhao et al. [18] also reported an analysis of the flexible rotor, following the model of Figure 6(b), with the aim of illustrating a more general methodology. Leaving aside the goal of an effective parametric characterization of the system, operating conditions with medium unbalance and low damping were assumed in the study. An analytical approximated expression of the equations of motion was adopted with the use of trigonometric series (the same approach was given to the study of both rigid and flexible *uncentralized* rotors; see sections 3.2 and 3.3). The coefficients of the series represented the solution of a nonlinear algebraic system of equations, sought by means of the *trigonometric* (sometimes *time*) *collocation method* (*TCM*) [23, 24]. Obviously, the hypothesis of centralized rotor with SCCOs allowed a simplification of the series. Thus, the amplitude-frequency response was obtained through determination of the harmonic components of the series as a function of the rotor speed (an *arc-length continuation algorithm* was adopted at this stage, according to the indications from [25, 26]). An example of such a response is illustrated in Figure 10(a), where the authors compared their data with those from [16] (the same parameters were assumed). Investigation of solution stability was carried out by examining the Floquet multipliers. During the application of the Floquet theory, the transition matrix was approximately evaluated by means of the *rectangular ripple method* [27]. With reference to the solutions illustrated in Figure 10(a), the corresponding variation of the first multiplier with the rotor speed was depicted in Figure 10(b).

Points a, b, c and d in the latter figure correspond to points A, B, C and D in Figure 10(a), respectively. The top diagram, relative to the modulus of the multiplier, clearly shows the instability of the solution along the middle branch AB and the segment CD of the response curve. The variation of the real and imaginary parts of the multiplier, in the middle and bottom diagrams, suggests that a saddle-node type of instability affects the solutions along AB (where jump phenomena at the critical points occur). From the same diagrams it can be inferred that a leading pair of complex-conjugate multipliers regulates the instability of the solutions along the CD section, where the periodic motion bifurcates (secondary Hopf bifurcation) into a quasi-periodic one. The results obtained with the above procedure, from the standpoint of bifurcation theory, were compared with the data from direct numerical integration of the equations of motion.

Gunter et al. [21] carried out stability analysis in order to optimize the design of the SF-supports for a centralized flexible rotor, with mass at midspan and supports, in the presence of *aerodynamic force* (*cross-coupled stiffness force* or *Alford's force* [28]). Stability maps were obtained with distinct values of the aerodynamic force, under the hypothesis of small journal eccentricities, so as to reasonably assume constant characteristics for the fluid film (i.e. stiffness and damping coefficients) that were determined with the SBA. Despite the adopted simplifications, the maps show that either high stiffness or low damping in the supports gives rise to rotor instability. The regions of stable operation made it possible to evaluate the optimum stiffness and damping for suitable design of the dampers. Further examples were given with direct numerical integration of the equations of motion for a model of a turborotor on tilting-pad bearings (internal friction was assumed here, in place of the aerodynamic force, as the *additional destabilizing factor*) and experimental tests of a centrifugal compressor (in the presence of aerodynamic force varying with the level of the discharge pressure). Data from both the examples show the ability of SFDs to stabilize the motion.

3. Extensions of the Basic Models

The above models of rotor-support systems are to be changed when:

- The investigation is broadened to include the possible onset of nonsynchronous whirling motions, keeping unchanged the symmetry of the rotor, the isotropy of supports and the hypothesis of CCOs.
- The above hypotheses about the rotor and the supports are removed and/or a static journal eccentricity results because the centering suspension system is imperfectly adjusted or absent, in the presence of a unidirectional load.
- A better approximation of the dynamics of the actual rotor is sought through the adoption of a multi-DOF model consisting, for instance, of a lumped model of the rotor, with a certain number of masses, *linear* supports and *nonlinear* supports (the latter represented by the supports with SFDs). In the extended model, the simplifying hypothesis of centralized mount of the dampers, with SCCOs of the journals in the respective bearings, is held.
- The previous case is generalized by removing the hypotheses of ideal centering of the damper journals and SCCOs.
- Particular aspects, roughly approximated or wholly neglected in the elementary models of rotor-supports system, are investigated. Lubricant inertia, cavitation in the film, the sealing and oil supply, the geometry of the damper, the flexibility of the housing, and other aspects may greatly affect rotor dynamics and consequently deserve attention by means of a suitably extended model. Improvements in the design of the dampers can also motivate an extension of the basic models.

3.1. Centralized Rigid Rotor with Nonsynchronous Orbits

A first generalization of the rotor described by means of equations (1) is obtained after removing the SCCO hypothesis. The journals of the rotor are assumed statically centered in the respective bearings of the dampers. With reference to Figure 11, the equations of motion are:

$$\begin{cases} -M(\ddot{e} - e\dot{\varphi}^2) + Mu\omega^2 \cos(\omega t - \varphi) - ke - F_r = 0 \\ -M(e\ddot{\varphi} + 2\dot{e}\dot{\varphi}) + Mu\omega^2 \sin(\omega t - \varphi) - F_s = 0. \end{cases} \quad (4)$$

The reference rotates in accordance with the motion of precession of the rotor, at the angular frequency $\dot{\varphi}$, distinct from the given constant angular speed ω of the rotor.

This model was analyzed by Li and Taylor [29] by numerically integrating the equations of motion, with use of the πSBA for expressing the SF-force. This investigation, carried out after the usual adoption of the B_n, ω / ω_n and U

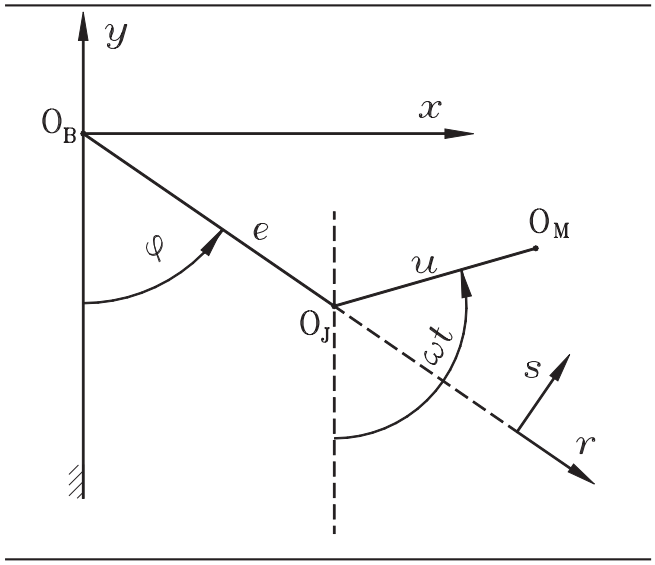

Figure 11. Relative positions of O_B, O_J, and O_M for the rigid rotor, with generic orbits of O_J

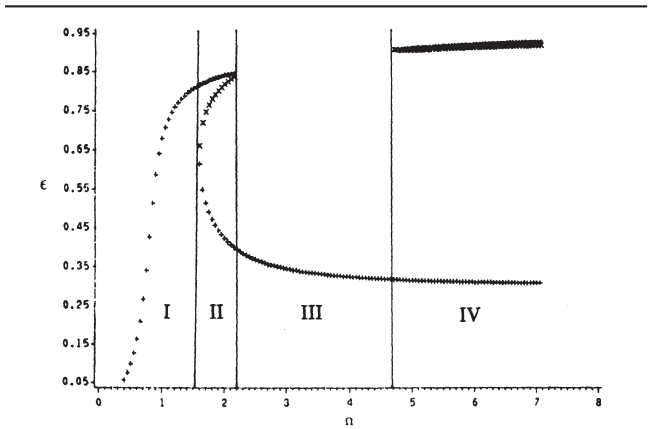

Figure 12. Theoretical response (synchronous solutions) for the unbalanced rigid rotor, obtained with fixed values of the unbalance (0.3) and bearing parameter (0.072), under π-film conditions. Besides the synchronous solutions, nonsynchronous motions can occur in regions III and IV of the eccentricity ratio ε vs. speed parameter Ω plane (reproduced by permission of the ASME [29])

parameters (different symbols were adopted in the cited paper), showed the existence of quasi-periodic motions of the rotor, under conditions characterized by low values of the bearing parameter (the value of 0.072 represents operating conditions for the rotor in the presence of low lubricant viscosity and/or high angular speed). This quasi-periodic character was attained by the whirling motions in the regions III and IV of the amplitude-frequency response (Figure 12). In these intervals of the angular speed, a quasi-periodic solution co-exists with one (region III) or two (region IV) synchronous solutions. A qualitative indication about the probability of existence for each of the possible solutions was inferred by examination of the *basins of attraction,* showing the influence of the initial conditions about the onset of either motion. Further indications were obtained through an inspection of the topological structure of the system and the root locus relative to the local motion about the synchronous stable orbits. The higher or lesser degree of attraction of the orbits itself was dependent on the amplitude of the real part of the complex characteristic roots. Weak attraction of the synchronous orbits, in the above cited III and IV regions, corresponded to the small real part of the complex roots and made nonsynchronous solutions likely to arise.

3.2. Rigid Rotor in the Presence of Static Eccentricity and/or Dissymmetry

Some extension of the basic model for analysis of the rigid rotor, given in section 2.1, was achieved with the inclusion of conical motions. Such a generalization was motivated, for instance, in [8, 10], by the need for treating the case with rotor on unequal supports, with particular reference to the arrangements where only one of the two supports was mounted with SFD.

This condition, realized in the experimental rig of Simandiri and Hahn [10], as well as in other rigs, was preferred to the equal supports-solution in order to cut off the influence of possible unpredicted deviations, at the experimental stage, from the theoretical symmetric scheme. In the paper, the measured data were compared with the theoretical predictions obtained from two equations of motions, written under the hypothesis of SBA and SCCOs. Thanks to suitable changes given in the expression of the parameters, these equations could be referred, in the same form, either to the case of equal end SF-supports (cylindrical symmetric motion) or to the case of SF-support plus a self-aligning bearing-support (conical motion with apex of the cone at the self-aligning bearing-support). A *pressure parameter*, as in [11], allowed management of conditions characterized by non-atmospheric supply pressure. For unpressurized conditions, the predicted dependence of the jump speed on the unbalance parameter and the bearing parameter was experimentally confirmed along with the existence of a *jump-free region*. The absence of jump for pressurized conditions was also confirmed. The effect of different values of the supply pressure on the size of the journal orbit was observed, while no attempt was made to evaluate the transmissibility.

A more general, design-oriented, organization and presentation of the data relative to the steady-state vibration amplitude and transmissibility, in unloaded vertical rotors and centrally preloaded rotors, was given in the theoretical paper of Hahn [8]. The model of rotor-support system was the same as that used in [10], and a particular combination of the parameters was carried out for presenting the data (in a general form suited for either cylindrical or conical motions). Among other things, the results illustrated, besides confirming the indications from previous investigations, that a negligible difference exists between the behavior of unloaded vertical and centrally preloaded rotors.

Some asymmetry also affected the model adopted by Cooper [30] for his well known experimental investigation (see also [1]), that was carried out with a rigid rotor test rig, mainly consisting in a shaft carrying two wheels, on two supports initially fitted with gas bearings and later with ball bearings. The analysis suitably shed light on the beneficial use of SFDs. A significant part of the work was devoted

to testing the capability of different means (bumpers, limiting ring, hydrodynamic journal bearing in conjunction with sprung gas-bearing) in vibration control. Throughout the tests, unsymmetrical arrangements of the horizontal rotor were set. In fact, the unbalancing of the rotor was achieved through imbalance given to a single wheel and operations aimed at testing different solutions for vibration control regarded a single half of the system. The dynamic behavior was experimentally characterized in terms of amplitude of vibration, acceleration of vibration and phase angle between the displacement and the unbalance. Among the different solutions for improving the rotor response at resonance, the best results were achieved with the combination SF – ball bearing – coil-springs in parallel mount to the SF (see Figure 2 in [1]). The bearing of the damper was realized with two lands separated by a central circumferential groove. Three examples of dampers were reported, respectively realized with different combinations of land widths and radial clearances. In all three cases the damper was effective at the main resonance (a further resonance was observed at higher speeds). Nevertheless, the results showed the need to avoid too small radial clearances (in this case, no inversion was observed at the highest unbalances) and too high land widths (the journal orbits tended to cling to the periphery of the bearing, as an effect of the instability of the initially eccentric small orbits). The role of the oil supply and that of oil viscosity represented further aspects investigated in the course of the experimental tests. In particular, the increase in the tangential component of the SF reaction and the corresponding decrease in the radial component, as a consequence of raising the supply pressure, were observed.

Further reasons for extending the basic model of section 2.1 stem from the inadequacy of the SCCOs hypothesis in treating those conditions characterized by a static eccentricity of the damper journals. The *deficiency* of symmetry, in the system of forces acting on the journal, makes its trajectories diverge from the centered circular motion, and increases the likelihood of nonsynchronous behavior.

Eccentricity in the journal static position is due to the absence of retainer springs (in the presence of side load acting on the rotor, the static eccentricity of the journal corresponds to the whole clearance in the bearing) or, alternatively, in the presence of elastic suspension, to an imperfect centering of the journal. The latter condition, represented by a *residual* static eccentricity, is mainly dependent on the characteristics of the retainer springs and/or the presence of unidirectional load, perpendicular to the rotor axis. Unequal stiffnesses in the elements of the elastic suspension give rise to static eccentricity in the absence of unidirectional loads (unloaded vertical rotor). By contrast, when such a load is present, poor regulation of the same elastic elements makes the journals of the rotor uncentered in their respective bearings.

The weight W of the rotor (*normally*, for horizontal disposition of the rotor, the sole unidirectional load, perpendicular to the rotor axis, that is responsible for the above static eccentricity) is generally expressed as a dimensionless *gravity parameter* $\overline{W} = W/(MC\omega^2)$ or $\overline{W} = W/(MC\omega_n^2)$. The latter ratio can obviously be adopted on condition that the SF supports are equipped with retainer springs whose stiffness is $M\omega_n^2$. It is worth noting that, in the absence of

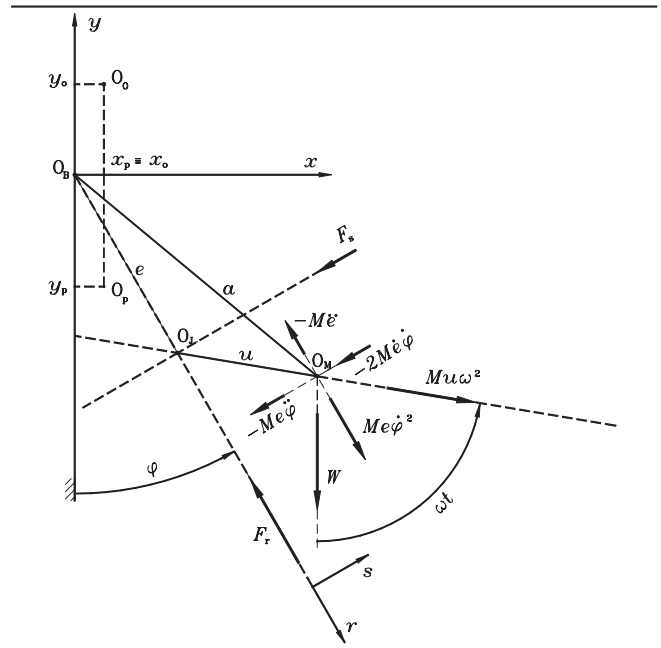

Figure 13. Scheme for the study of the rigid rotor in the presence of static eccentricity and gravity load. O_0: position of the journal center that is only due to the preload of the centering springs, in the absence of gravity load W; O_p: position of static equilibrium of the journal center; O_J: actual position of the journal center

springs, the gravity parameter explicitly appears in the equation of motions of the horizontal rotor. Conversely, in the presence of springs, in the equations of motions, normally written in the usual references with the *origin coinciding with the bearing center*, a component of the static load, that corresponds to the static eccentricity, explicitly appears as a *gravity residual* (see below in the present section).

When the rotor is supported on SFDs without centering elements and the rotor-supports system is symmetrical with respect to its middle plane, the equations of motion in the coordinates r and s of Figure 13 can be written as (with reference to the half-rotor, in accordance with the assumed symmetry):

$$\begin{aligned} &-M(\ddot{e} - e\dot{\varphi}^2) + Mu\omega^2 \cos(\omega t - \varphi) + W\cos\varphi - F_r = 0 \\ &-M(e\ddot{\varphi} + 2\dot{e}\dot{\varphi}) - Mu\omega^2 \sin(\omega t - \varphi) - W\sin\varphi - F_s = 0. \end{aligned} \tag{5}$$

In the presence of elastic elements, with k denoting the stiffness of the suspension per each support, $(x, y) \equiv (e, \varphi)$ the coordinates of O_J, and $(x_p, y_p) \equiv (e_p, \varphi_p)$ the coordinates of the center of the journal in the position O_p of static equilibrium, equations (5) are replaced by:

$$\begin{aligned} &-M(\ddot{e} - e\dot{\varphi}^2) + Mu\omega^2 \cos(\omega t - \varphi) \\ &\quad - k(\Delta_x \sin\varphi + \Delta_y \cos\varphi) - F_r = 0 \\ &-M(e\ddot{\varphi} + 2\dot{e}\dot{\varphi}) + Mu\omega^2 \sin(\omega t - \varphi) \\ &\quad - k(\Delta_x \cos\varphi - \Delta_y \sin\varphi) - F_s = 0 \end{aligned} \tag{6}$$

with: $\Delta_x = (e\sin\varphi - e_p \sin\varphi_p)$ and $\Delta_y = (e\cos\varphi - e_p \cdot \cos\varphi_p)$, or equivalently, assuming the coordinates x and

y, with $-F_x$ and $-F_y$ denoting the components of the film force, by:

$$\begin{aligned} -M\ddot{x} + Mu\omega^2 \sin\omega t - k\Delta_x - F_x = 0 \\ -M\ddot{y} - Mu\omega^2 \cos\omega t - k\Delta_y - F_y = 0 \end{aligned} \tag{7}$$

where:

$$F_x = \frac{xF_r - yF_s}{\sqrt{x^2+y^2}}, \qquad F_y = \frac{yF_r + xF_s}{\sqrt{x^2+y^2}}, \qquad \Delta_x = x - x_p,$$
$$\Delta_x = y - y_p.$$

In Figure 13, the coordinates x_0 and y_0 indicate the position of the journal that is only due to the preload of the centering springs, in the absence of W. The difference $y_p = y_0 - W/k$ represents the component of the *static eccentricity* of the journal, along the vertical direction, owing to the action of the gravity load. This component (or the product $ky_p = ky_0 - W$) is sometimes indicated as *gravity residual* and expressed in dimensionless way by means of the ratio y_p/C. Interestingly, in the absence of elastic suspension, the residual unbalance of the rotor is generally sufficient to make the journal lift up from the bottom static position within the bearing.

Analysis of the above model was tackled in [4, 17, 29, 31–37]. In particular, analytical approximated solutions were reported in [4, 34]. The circular orbits corresponding to a given rotor imbalance were perturbed with the application of the static load. The linear differential equations of the perturbed motion were solved under the hypothesis of synchronous response and with the assumption of linearized stiffness and damping coefficients [1] for the expression of the film force. Apart from the film model, the above coefficients were dependent on the radius of the circular orbit and, in turn, on the level of unbalance.

White [4] obtained (under the πSBA) a diagram that put the radius of the approximated orbits in correspondence with the product of the dimensionless *gravity load* by the reciprocal σ of the bearing parameter, for rotor conditions characterized by the absence of the retainer springs. An acceptable comparison with the results of the numerical approach was found until the radius of the linearized circular orbit was less than one third of the radial clearance. Further, a separate illustration of the orbits numerically obtained with variation of the gravity load and the bearing parameter, in the presence of a fixed value of the rotor unbalance, was reported. The tests showed that the presence of a static load could make the inverted orbit change to an uninverted one, in addition to determining, in some cases, the onset of nonsynchronous orbits with a main frequency component in a ratio that was about 1/2 of the driving frequency.

Holmes and Sykes [34] determined the eccentric approximated circular orbits of the journal centre with different values of the unbalance parameter (u/C) and the dimensionless static load ($W/(MC\omega^2)$). The analysis was carried out both in the absence and presence of retainer springs (the dimensionless stiffness was represented by means of the parameter $K/(M\omega^2)$). The results respectively obtained with both the above procedure (with use of the πSBA and the relative coefficients) and the integration of the full nonlinear equations showed good agreement, that improved significantly in the presence of elastic elements and with the highest unbalances. The authors stressed the limits to the simplified treatment of cavitation and the existence of speed ranges affected by subharmonic motions.

The approximated analytical approach was also a distinctive feature of the analysis of Pan and Tonnesen [32]. The motion of the unbalanced rigid rotor, in the presence of gravity residual, was characterized through perturbation of the eccentric orbits of the journal. The authors, at a preliminary stage, showed that further components of the film force, in addition to the fundamental, synchronous component, arise as a consequence of decentralizing the synchronous circular orbit that is due to rotor unbalance. In particular, besides the synchronous component of force, prominence is to be given to the second order component and to the constant term, that represents the *lift off* (null for 2π-length of the film). The presence of the secondary components of the fluid film force determines, in turn, the excitation of nonsynchronous, periodic components of motion. These remarks were applied to the analysis of steady motion of the rotor, represented by an eccentric orbit of the journal, that was perturbed with a second order component. The corresponding film reaction, in accordance with the above observations, was approximated by means of the constant component plus the synchronous and second order ones. Simple relationships were assumed between the components of motion and those of the film force, with a limitation of the cross coupling between the components of motion and force, having different orders (*temporal orthogonality condition*). In this way, Pan and Tonnesen obtained some examples of orbits that were characterized by different degrees of eccentricity and distortion, depending on the value assigned to the gravity load. Further data (for cavitated film conditions) showed the occurrence of jump in the presence of high rotor unbalance (the characterization of the jump phenomena was less detailed than in other investigations) and an increase in the *lift off* of the journal orbits with the rotor speed.

In the other cited investigations regarding the model of rigid rotor affected by static eccentricity, the approach was numerical or analytico-numerical. Gunter et al. [31] reported some theoretical examples where the journal orbits were numerically determined (*time transient analysis*) in the presence of unidirectional load (static load). The rotor was assumed to be equipped with retainer springs but not centrally preloaded, or devoid of retainer springs. In the first case, the influence of different values given to the stiffness of the elastic suspension (and consequent different gravity residuals) was tested. The transmissibility of the system in the above conditions was evaluated, taking into account medium-high unbalances and different values of the supply pressure (in order to determine full cavitated or uncavitated lubrication regime in the dampers). Analysis highlighted the negative role of the unidirectional load, as far as the transmissibility (examples with values up to about 7 were reported) and the onset of non-periodic motions were concerned.

Cookson and Kossa [33], by means of numerical integration of the equations of motion, performed an analysis that pointed out the role played by the static load as regards the efficiency of the dampers. In particular, values of the gravity parameter $\overline{W}$ suitably limited (not above a limit of about

0.1) were still compatible with good operation of the dampers. With the increase in $\overline{W}$, an unacceptable amplification of the force transmitted to the supports from the unbalanced rotor was found (examples with $\overline{W}$ = 0.4, 0.6). The results of the study also showed the importance of assigning adequate values for the bearing parameter, not so high (and less than 1.0 in any case), on the one hand, so as to avoid the "*lock-up*" of the dampers, nor too low (a limit of 0.1 could reasonably be assumed) on the other hand, in order to avoid the onset of nonsynchronous whirling motions. An experimental investigation substantially confirmed the predictions of the theoretical model, though evidencing some limits probably due, among other things, to the approximation (πSBA) adopted for the damping film.

Hahn and Chen [17] theoretically determined the eccentric orbits of a rigid unbalanced rotor, with no centring springs, making use of the HBM supported by an iterative numerical routine (Newton–Raphson) for solving the nonlinear algebraic system. The reported examples show that the convergence of the procedure was dependent on the number of the terms adopted for the harmonic series (7÷11 terms turned out to be sufficient). In this respect, a suitable comparison with the results of the direct numerical integration of the differential equations of motion was made. In this analysis the πSBA was adopted for describing the SF behavior.

Li and Taylor [29], in addition to the results given for the centralized rotor with low values of the bearing parameter (B_n = 0.072), showed that the precession motions of the unbalanced rotor can attain synchronous or sub-harmonic character (with frequencies that are in ratios of 1/2, 1/4 and 1/6 with respect to the driving frequency) when the gravity residual is not negligible and comparable with the unbalance parameter (in the example the static eccentricity was set at 0.7). Under these circumstances, analysis showed that, changing from the centralized rotor case to that with static eccentricity, while maintaining the other conditions unchanged, the sub-harmonic nature of the motion *de facto* takes the place of the nonsynchronous character. By contrast, small values of the gravity residual make the motion of the rotor similar to that obtained for centralized conditions, with orbits of the journal that are not very eccentric with respect to the bearing center.

Zhao and Hahn [35] studied the system with the same set of parameters adopted by Li and Taylor [29], i.e. fixing a medium value for the static eccentricity, a moderate damping at the supports and a medium/high rotor unbalance. The data obtained by numerically integrating the equations of motions suggested the existence of speed ranges in which the motion was subharmonic (orders of 1/2, 1/3, and 1/6), quasi-periodic or chaotic. The results of the investigation were summarized by means of two bifurcation diagrams obtained with speed increase (Figure 14(a)) or decrease (Figure 14(b)), respectively, and starting with different initial conditions. Both figures make it possible to infer the existence of jump phenomena at low speed, in accordance with the results given in other investigations. The variety of different motions was strongly dependent on the initial conditions selected for numerical integration. Subharmonic, quasi-periodic and chaotic solutions are present at speeds that correspond to zones III and IV of the analysis reported in [29].

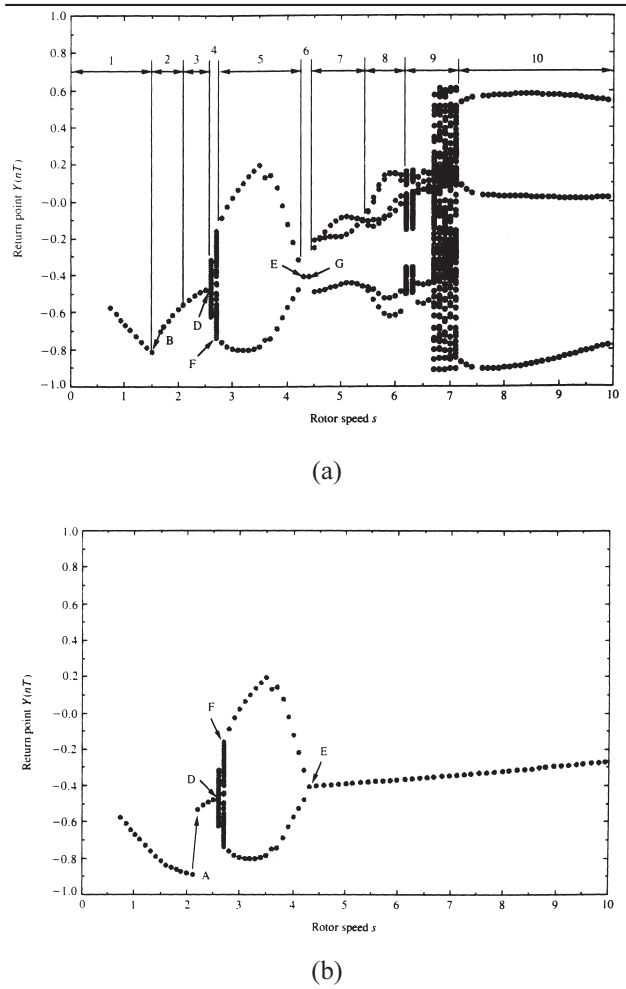

Figure 14. Bifurcation diagrams relative to the analysis of the rigid rotor behavior (static eccentricity, bearing and unbalance parameters were respectively given the values of 0.7, 0.072 and 0.3). The return points $Y(nT)$ were plotted as a function of the speed parameter s: (a) diagram obtained with speed increase; (b) diagram obtained with speed decrease and suitable set of initial values for numerical integration (this material has been reproduced from [35] by permission of the Council of the Institution of Mechanical Engineers).

The same case was reported by Zhao et al. [37] who carried out their analysis by means of the TCM and the Floquet method, in line with the study referred to in section 2.2 [18]. The data obtained with this procedure were compared with those from numerical integration of the equations of motion. The amplitude-frequency responses relative to some of the terms in the trigonometric series adopted for the approximated solution, highlighted the fact that jumps occur not only with a sudden change in the size of the orbit covered by the journal centre, but also with a change in the relative position of the orbit with respect to the bearing. Two orders of approximation for the solution – respectively with four and eight harmonic terms of the series – were further compared. The results were congruent with those from other studies (in particular [29]) and showed the instability of the synchronous solution and the consequent presence of sub-harmonic motions (with 1/2 ratio) in the interval of the operating speed at about twice the natural

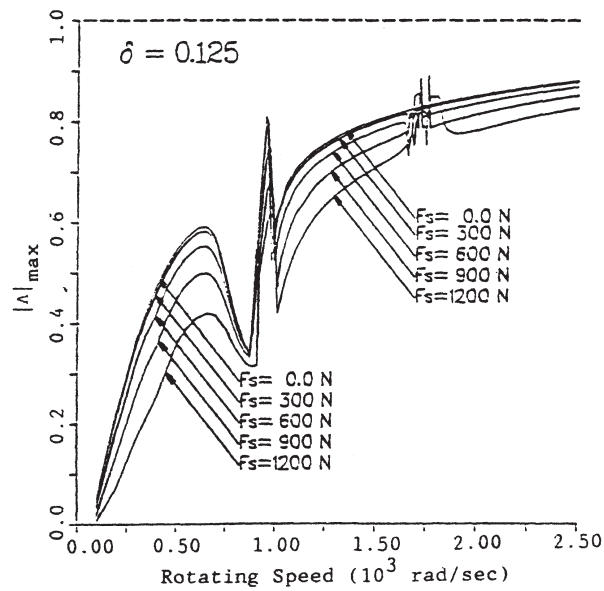

(a)

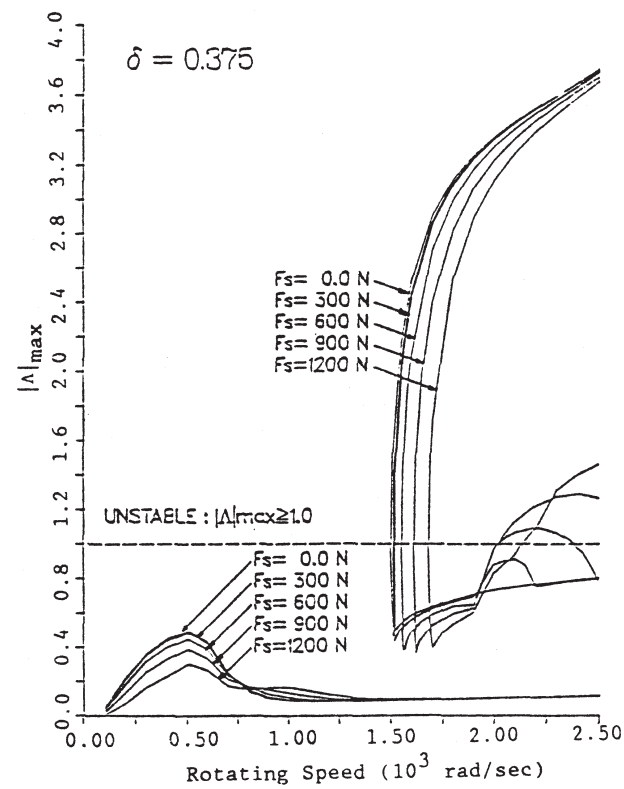

(b)

Figure 15. Stability maps (maximum absolute value $|\Lambda|_{max}$ of the eigenvalues of the transition matrix vs. speed parameter) for different values of the unbalance parameter (δ) and side load F_s: (a) δ = 0.125; (b) δ = 0.375 (reproduced by permission of the ASME [36])

frequency ω_n. In a further case, characterized by higher static eccentricity, the unstable character of the synchronous solution was found persistent approximately in the same region. Analysis of the Floquet multipliers indicated that, with increases in speed, the instability of the synchronous solution gave rise to successive bifurcations respectively representing changes to quasi-periodic and sub-harmonic motion (with period doubling), before the synchronous nature of the solution was regained at higher speed. Nevertheless, under the assigned operating conditions, characterized by a remarkable nonlinearity that was due to the high static eccentricity, the investigation also underlined some limits to the analytico-numerical approach. The need for a solution that was reasonably approximated and suited to the variety of the dynamic responses of the system led to the adoption of trigonometric series with high numbers of terms, thus unavoidably making the procedure more involved. Nonetheless, the same series proved completely inadequate for expressing non-periodic behavior of the rotor. These considerations suggested recourse to direct numerical integrations of the equations of motion as a support to the approximated analytico-numerical approach. Despite the relative robustness of the numerical integration procedure, some difficulties arose in the search of solutions for eccentricities close to one, in the region with bistable behavior, downstream of the jump-up (for run-up operation).

An approach that makes use of the *hybrid numerical method*, a technique stemming from both HBM and TCM, was adopted by Shiau et al. [36]. The authors examined the model already studied by Taylor and Kumar [9], after addition of a side load (equivalent to a gravity residual), for the illustration of the analytico-numerical technique illustrated in [38] (section 3.4) and further extended here to the study of stability, with recourse to the Floquet method. The results illustrated the influence of the side load on the speed corresponding to the onset of jump and made it possible to infer the role played by the same load in destabilizing the low-eccentricity, synchronous solution that set in after jump (for run-up operation). This instability gave rise to a sub-harmonic response, in speed range placed at about twice the critical speed, and the thresholds of instability, for different levels of the side load (Figure 15), were determined. In some cases, the orbits obtained through the analytic-numerical procedure were compared with those obtained from the numerical integration of the differential equations.

3.3. Flexible Rotor in the Presence of Static Eccentricity and/or Dissymmetry

A mathematical model, similar to that of the above section, can be given for the analysis of the dynamic behaviour of the flexible rotor. Examples of investigations relative to this case, with the rotor affected by static eccentricity, were given in [4, 17, 18, 39–42].

White [4] studied the flexible rotor with mass at mid-span, vertical disposition and *side load*, in the absence of centering elastic suspensions equipping the SFDs, as in the analysis carried out for the rigid rotor and referred to in the above section. The perturbation approach ruled out the role played by rotor flexibility and the results coincided with those relative to the rigid rotor case.

Cookson and Kossa [39] analyzed a model of symmetric flexible rotor with mass at mid-span and supports, with horizontal axis and SFDs devoid of elastic suspensions. A set

of different values for the gravity parameter was assumed with the aim of taking due account of different arrangements and combinations of load and radial clearances. The data obtained by numerically integrating the equations of motion in a speed interval below the second critical speed, with the SF force expressed by means of the πSBA, indicated how the incorrect design of the SFDs in the rotor-support system might give rise to anomalous operating conditions and especially to high values of the transmissibility (see Figure 3 in [1]). The results further confirmed that the adoption of well designed dampers, on the contrary, turns out to be an efficient means of limiting the effects of rotor unbalance, provided that the gravity parameter, the bearing parameter and the mass parameter are given values that are suitably limited.

Saito [41] applied the HBM to the analysis of a symmetrical flexible rotor with mass at mid-span, in the absence of centering elastic suspensions at the SF-supports. The SF behavior was described by means of the πSBA and a unitary value was assigned to the gravity parameter. The effect of different levels of rotor unbalance was observed, with restriction to the synchronous response. In particular, depending on the zone of the interval of speed, the verse of speed variation and the level of unbalance, four different kinds of synchronous motion were found, one of which proved extremely sensitive to the unbalance.

Zhao et al. [18] adopted conditions represented by a medium-high value of the static eccentricity of the journals, in a case that was reported in addition to the theoretical analysis for *centralized* operation (section 2.2). Four harmonic terms, besides the constant one, were taken for the trigonometric series that expressed the approximated solution (according to the TCM). The reported data (obtained with use of the πSBA) illustrated the presence of a zone where the instability of the synchronous solution occurs (as inferred from inspection of the largest Floquet multiplier), in addition to the two instability-regions already detected in the centralized case (Figure 16(a)). In this range of the operating speed (segment EG in figure) the synchronous solution bifurcated into a sub-harmonic motion of half order as confirmed by the orbits (Figure 16(b)) obtained both through numerical integration and the analytico-numerical procedure (a comparison of the results is carried out in the figure). The character of the same motion was also evidenced by the Poincaré map (Figure 16(c)).

An analogous model had been examined by Shiau and Jean [40] as an application of a more general approach (section 3.4). The results of the investigation carried out by adopting the HBM with a four harmonic-approximation suggested that the higher the static eccentricity, the more evident the excitation of higher components of the approximated solution.

The *Floquet transition matrix method* was also used by Zhang et al. [42] for theoretically investigating the stability of motion of a symmetric flexible rotor, arranged horizontally. In the SF support at either end of the shaft, a plain journal bearing was adopted in series to the SF, as the inner member of the damper, instead of the more common roller or ball bearing. The πSBA and the πLBA were respectively employed for expressing the fluid forces in the SFD and the journal bearing. The mass of the rotor was placed at the mid-span and at the two supports. In particular, the aliquot

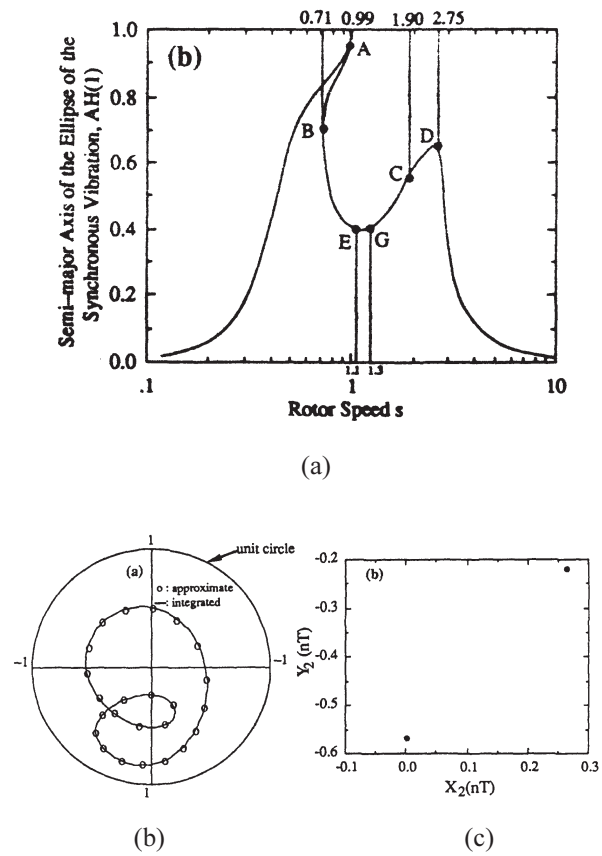

Figure 16. Theoretical response relative to the flexible rotor in the presence of static eccentricity (fixed equal to 0.5; the bearing parameter was 0.06 and the other parameters were assigned as in Figure 9(b)): (a) semi-major axis of the ellipse of the synchronous vibration vs. speed parameter, with indication of the instability zones; (b,c): orbit and Poincaré map relative to a sub-harmonic motion in the interval of speed corresponding to the segment EG in (a) (reproduced by permission of the ASME [18])

of mass at each bearing station was separated into a journal (inner) mass and a bearing mass. The bearing was connected to the outer fixed ring of the damper with an elastic suspension, parallel to the SF. The resulting twelve first-order differential equations of motion were numerically integrated for unbalanced and well-balanced rotor conditions, with further examination of the Floquet multipliers. Three examples of bifurcation were reported – obtained for different sets of the parameters, respectively, at varying the rotor speed – and illustrating, with reference to the position of the bearing center, an equilibrium point bifurcating into a limit cycle (Hopf bifurcation), and a periodic motion into a quasi-periodic or a period-doubling motion.

Models with nonsymmetric rotors were examined in [17, 43–45]. Botman and Samaha [43] experimentally examined the dynamic behavior of a rotor with an overhung disk. Both supports were provided with SFD and only one was equipped with retaining springs. In the course of the tests, the rotor was run, after suitable balancing (carried out with the modal technique), in the speed range including the first two critical speeds. The occurrence of half-order sub-harmonic whirling was observed at approximately twice the first critical speed. *Jumps* were also observed during the tests and the

effectiveness of pressurization as a means of suppressing this phenomenon was experimentally confirmed.

In [17] the study was reported in order to give a further instance of a general methodology based on the HBM (see sections 3.2 and 3.4) and dealt with a six DOF rotor on two supports, the one with SFD and centering springs and the other rigid and equipped with self-aligning ball bearings. The mass of the rotor was mainly represented by a disk at mid-span, while a minor part was placed at the supports. The gyroscopic terms related to the inertia of the disk and both static and couple components of the disk unbalance were introduced into the equations of motion. A comparison between the theoretical and experimental amplitude-frequency responses, for centralized conditions, showed the occurrence of jump phenomena for operation close to a resonant speed of the system. The conditions in the absence of centralizing springs parallel to the SFD were also dealt with and some examples of the theoretically obtained orbits covered by the centre of the journal were reported. Some experimental data was also reported.

A horizontal unsymmetrical flexible rotor, realized following the arrangement that was typical of the rotors of small centrifugal pumps, was analyzed by Chu and Holmes [45]. A disk overhung mounted with respect to the unequal supports, only one of which was equipped with SFD and centering springs, represented the main mass of the rotor. Part of the analysis was carried out experimentally and effectively showed that high levels of the static eccentricity assigned to the journal in the SFD, the disk unbalance and the supply pressure determined separately excessive damping in the SFD and a shift in the frequencies of the resonant peaks of the system. As a consequence of the excessive damping, the effectiveness of the centering suspension was limited and the dynamic response was close to that obtained with rigid supports. A further part of the study addressed the theoretical analysis of the effect of SFDs on rotor stability. In this regard, the operating conditions for real rotors of centrifugal pumps were simulated by including an annular seal in the mathematical model of the rotor. The linear study, carried out by means of the *Direct Stiffness Method* and the determination of the eigenvalues of the system along the *Leonhardt locus*, indicated the beneficial role of the damper (here treated as a *linear* element) that increases the instability threshold with respect to the case of the absence of the damper. The dynamic behavior of the rotor beyond the above threshold was then characterized through numerical integration of the equations of motion. This part of the study regarding stability illustrated the ability of the damper, as an eminently *nonlinear* component, to make the rotor gain stability, thanks to the additional reserve of damping (with respect to a linear behavior) that allowed a *limit-cycle* to set in.

3.4. Multi-degree of Feedom Models

In several instances, the number of degrees of freedom (DOF) in the above models is too low in order to allow an acceptable approximation of the actual system and the relative dynamic behavior. Discretized, noncontinuous models for rotor bearing systems, with an extended, finite number of DOF, can be set-up with different techniques, so as to carry out the analysis with relatively simple lumped schemes, with a suitable number of masses and supports, and a a limited set of nonlinear elements (like the SF). Examples of investigations of rotors theoretically approximated with multi-mass or multi-degree of freedom (MDOF) models, were reported in [16, 36, 46].

These studies, leaving aside the scope of a parametric characterization of the dynamic response of the models under analysis, pursued rather the aim of improving well-established methodologies for *linear* analysis (FEM-based and others), so as to take due account of the nonlinearity resulting from a limited number of elements in the system, represented, in this context, by the SF-supports.

Greenhill and Nelson [46] analyzed the steady motion (represented by a precession synchronous with rotation) for a multimass flexible rotor, making use of an iterative technique stemming from the *secant method* for solving nonlinear equations. Once the *linear*, *algebraic*, *functional relationship* between the forces (mass unbalances and reactions at the supports) and the motion at the nodes of the discretized model was specified, the same relationship was adopted in an iterative way, in order to tackle the presence in the system of those *nonlinear elements*, like the SFDs, placed at one or more supports. It is worth noting that the original *differential* nature of the above functional relationship became *algebraic* after the hypothesis about the periodicity of motion. The iterative approach made it possible to *combine* the *linear skeleton* of the model and the *nonlinearity* of the SFDs. A first applicative example was reported with regard to a simple rigid symmetrical rotor. The iterative procedure outlined above, through a restricted number of iterations for each point, allowed the amplitude-frequency response to be obtained. A second example dealt with the rotor of a turbofan engine, with high pressure and low-pressure spools that were modeled with two different FE models, with 52 DOF and 84 DOF, respectively. In particular, three SF-supports were present. The system complexity raised the time for the calculus, with respect to the previous case, though leaving unchanged the average number of iterations at each step. A good performance of the procedure was verified, even under severe load conditions represented by *airfoil loss*. Nevertheless, limit conditions characterized by excessive journal eccentricities and particular distribution of the unbalances along the multimass rotor, with poor convergence and fluctuation of the solution, were observed, deserving the attention of the authors who indicated the need to check the physical significance of nonconvergence.

With respect to the above approach, later studies underlined the need to limit the computational burden connected to the iterative procedure. This aim was pursued by rearranging the original nonlinear model in two subsystems, one representing *the linear substructure* and the other the set of nonlinear components. This partition allowed a faster procedure with respect to that in [46] (an illustration of this approach was given in [24] together with a comparative discussion of the other methodologies for the analysis of nonlinear mechanical systems).

An example in this regard was represented by the analysis reported in [16], carried out under the hypothesis of synchronous whirl of the MDOF rotor, at constant angular speed. The procedure adopted in order to manage the nonlinearity of the system turned out to work with a number of equations that was greatly reduced with respect to the number of the whole equations written for the system,

with consequent benefit as far as efficiency was concerned. A further simplification can be achieved when the model of the rotor bearing system in question has a unique SF support (i.e. a pair of SF end supports for symmetrical arrangements). For such a case, an example was given with reference to the flexible symmetric rotor that had been already studied in previous analyses [12, 14] (see section 2.2). In this case, a biquadratic algebraic equation with dimensionless terms could be written. The solutions of the equation were collected as diagrams (B_n, ω / ω_c) obtained under fixed values of the eccentricity (see the example of Figure 9(a), with the relative comment on the symbols), and subsequently, customary (ε, ω / ω_c) curves were plotted (see Figure 9(b)). The procedure allowed the solutions for steady motion to be effortlessly determined, even in those regions characterized by the co-existence of more than one solutions, without the convergence drawbacks that affected some iterative methods. The stability of the steady solutions obtained with this procedure was investigated [13] through examination of the eigenvalues relative to the linearized equations written by perturbing the steady motion. This analysis showed that the stability results were independent of the presence of the unbalancing forces that incidentally act on one or more masses of the rotor, since the same forces did not appear in the equations of the perturbed motion.

In the presence of static eccentricities of the journals, periodic solutions which were not necessarily synchronous, were obtained by means of the HBM [17, 40] or the TCM [36]. The problem was tackled under a general approach, with indication of condensation procedures for suitably discretizing and substructuring the system and different algorithms for solving the nonlinear equations of motion. Nevertheless, most of the applicative examples reported in these studies were restricted to the simplest cases (already cited in section 3.3).

Shiau et al. [36] reported the analysis of a four-disk flexible rotor, on three supports, two of which were equipped with SFDs (Figure 17), as an example of the *hybrid numerical method*. The system of differential equations for the lumped model was set by means of the *general polynomial expansion method* (*GPEM*) [47] and solved with a procedure indicated in [38]. The paper reported the amplitude-frequency responses (semi major axis versus rotating speed) for the first two harmonics, relative to normal steady conditions, with nearly circular synchronous motion. An example of these data, with reference to station 3 of the model in Figure 17(a), is illustrated in Figure 17(b), where Shiau et al. separately obtained the curves with two different models (referred to in the figure and in [36] as equation (6) and equation (8)). The stability of the solutions was studied with the Floquet theory and a stability map was also reported.

With regard to eminent experimental studies, the examples of [22, 48, 49] can be mentioned at the end of this section. The experimental investigation of Cunningham [22] dealt with the dynamic behavior of a three disk symmetric rotor on a pair of end supports, equipped with SFDs and centering suspensions. With suitable unbalance given to each disk, different systems of unbalancing forces were obtained with a view to testing the ability of the dampers to attenuate the resonant modes of the system, paying attention to the fact that the effectiveness of the damping action

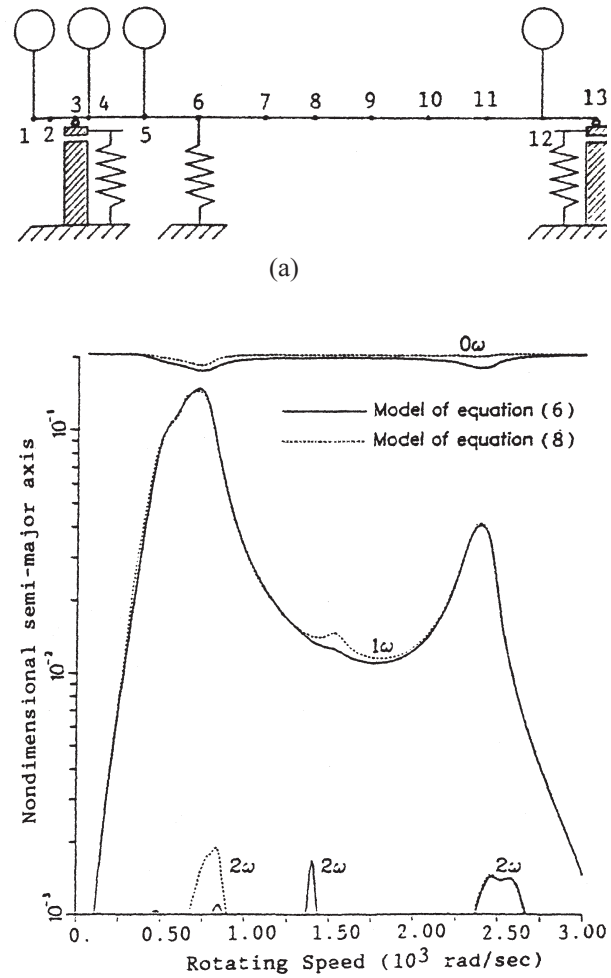

Figure 17. (a) Theoretical model of a multimass flexible rotor with rigid disks at stations 1, 4, 5, and 12, three linear isotropic supports at stations 3, 6, and 13, two SFDs with centering springs at stations 3 and 13; (b) first two harmonics of the amplitudes of the semi-major axis of the orbits at station 3, plus the orbits offset (equations (6) and (8) referred to in the figure are those reported in [36]) (reproduced by permission of the ASME [36])

depended, among other aspects, on the position of the dampers. The experimental data, after comparison with the theoretical predictions that were obtained under the πSBA, showed that the SFDs allowed considerable limitation of the vibration amplitudes and non-synchronous motions. The author mentioned further the occurrence of bistable behavior for operation characterized by severe unbalance, and conditions with possible starvation and rupture of the oil film within the dampers.

Kanki et al. [48] reported an interesting example of a field test regarding the effectiveness of SFDs for supporting multimass complex rotors. An industrial rotor representing one of the two rotational drive lines of a power unit, with two steam turbines (HP and LP) and a generator, with no SFDs in the rotor supports, exhibited a nonsynchronous vibration when operating under high-loading conditions (Figure 18(a) illustrates the theoretical model fixed up for

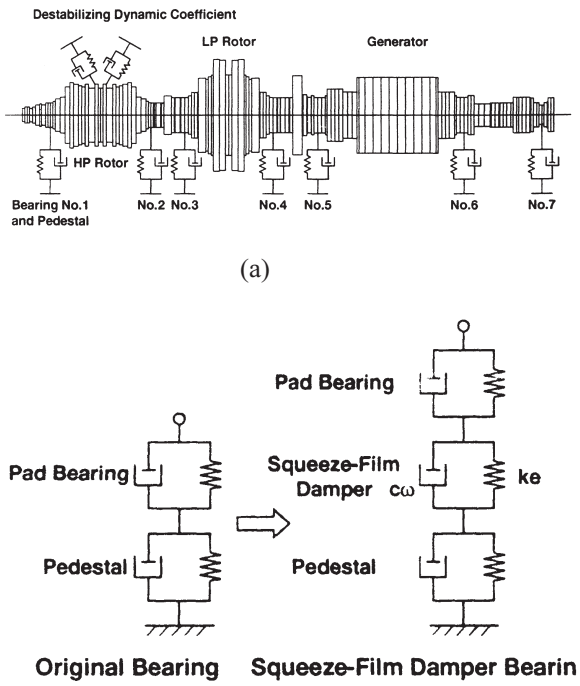

Figure 18. (a) Turbine rotor model adopted for the theoretical analysis with the transfer matrix method; (b) dynamic models of the rotor support before and after the adoption of the SFD (reproduced by permission of the ASME [48])

the rotor analysis). This vibration was identified as a steam whirl, originated by a sudden decrease in the damping ratio of the HP rotor first mode, presumably connected to the onset of stage excitation forces and labyrinth seal excitation forces. An experimental test, carried out with suitable excitation of the pad-bearing pedestal of the HP rotor, made it possible to assess the sudden change in the damping of the rotor first mode that proved unpredicted by theoretical analysis (transfer-matrix-method-based). The mounting of a single SFD within one of the HP rotor supports (support No.2 in Figure 18(a)), in series between the pedestal and the pad-bearing (Figure 18(b)), represented a valid remedy that made the nonsynchronous vibration disappear. In particular, the damper was designed according to the theoretical indications of Szeri et al. [50].

The paper of San Andres and Lubell [49] reported an instance of experimental parameter identification, relative to a nonsymmetric, three-disk rotor. The SFDs at the end supports were equipped with retainer springs and set (with seals) so as to make the fluid film behave in accord with the uncavitated model theoretically treated with the 2πSBA. In fact, a linear response for the unbalanced rotor was in practice obtained, even in the presence of medium-high damper values of the orbit radius, without the occurrence of jump and frequency-shift in the peaks of resonance corresponding to the different levels of unbalance. The system damping ratio, for different unbalance levels, was measured (by means of coast down tests) from the amplitude of vibration at resonance condition (system amplification factor relative to the first, pseudo-rigid, cylindrical mode), according to a result that is characteristic of the lightly damped systems. The corresponding values of the damping coefficients (vertical and horizontal directions) were thus calculated, taking account of the value of the critical damping, previously extrapolated after identification of the rotor-supports natural frequencies (different frequencies relative to the rigid cylindrical mode were found in the vertical and horizontal directions). The values obtained for the damping coefficients were compared with those calculated using the radius of measured orbits in the theoretical expression of the damping coefficient, written for the uncavitated short bearing model.

3.5. Models with Fluid Inertia, Cavitation, Sealing and Flexible-housing Effects

Particular aspects in the damper operation which have either been overlooked or only schematically treated in the models reported above, are capable of exerting an appreciable influence on rotor response. In this regard, the fluid inertia, the cavitation in the film, the characteristics of the feeding and draining of the damping film (supply pressure, geometry and position of the grooves or holes, presence of seals, etc.), and the flexibility of the frame integral to the supports (flexible-housing effect) have deserved particular attention in some studies. It is worth noting that some of the results illustrated here with reference to the dynamics of the rotor are to be correlated with results of the investigations specifically addressing the operating characteristics of the SFDs [1].

The influence of the inertia of the damping film on the dynamic behavior of the rotor has been investigated in [51–53]. The studies related to this aspect and referred to in Part I stress that the fluid inertia makes the damping capacity of the fluid film increase, with a rise in the tangential component of the film force and a reduction in the radial one.

San Andrés and Vance [51] carried out a theoretical study regarding both models of rigid and flexible unbalanced rotors, under the hypotheses of SCCOs of the journals and Re* (the modified Reynolds number, see Part I [1]) up to 20, with assumption of the πSBA and 2πSBA. As far as the unbalanced rigid rotor was concerned, the fluid film inertia was found to better the whole dynamic response, both for cavitated (π-film) and uncavitated (2π-film) conditions. The amplitude-frequency responses generally showed that, in the presence of inertia, the amplitude of rotor vibration was attenuated with respect to the case with Re* = 0, all other conditions being kept constant. In particular, the data relative to the π-film case underlined the role of inertia in the almost complete disappearance of the jump and the regions with bistable behaviour (Figure 19(a); the Reynolds number Rer in the figure was obtained from Re* by substituting the reference natural frequency of the retainer spring-rotor system ω_n, indicated here as ω_r, in place of the whirling frequency ω). The lack of the higher eccentricity branch along the responses was accompanied by a consequent advantage in terms of transmissibility (Figure 19(b)), even though this last aspect was negatively influenced when the increase in the fluid inertia was considerable (i.e. at higher speeds).

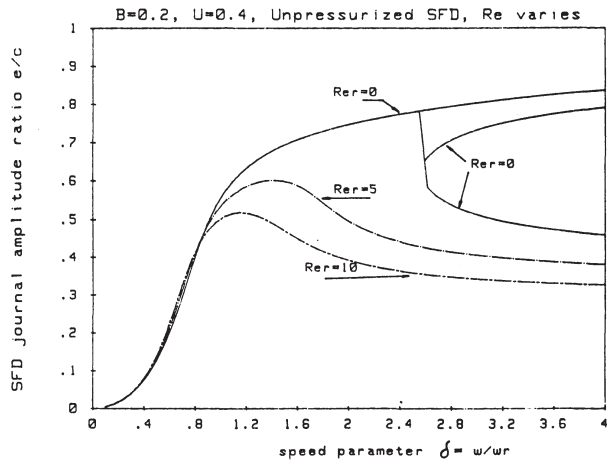

(a)

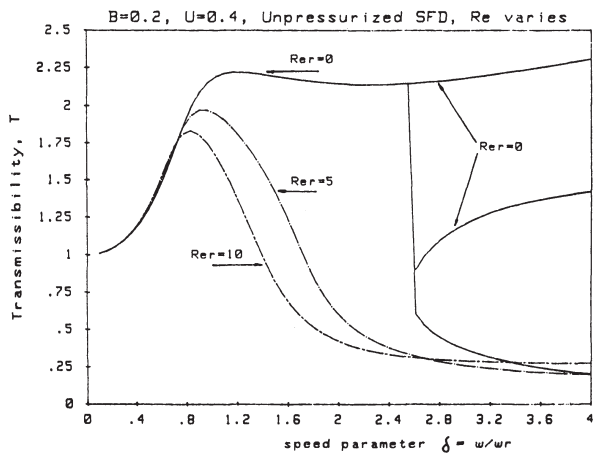

(b)

Figure 19. Theoretical frequency responses for the centralized, unbalanced rigid rotor, with unpressurized SFDs, in the absence of fluid inertia effects at the SFDs supports (Rer = 0) and with inertia effects (Rer = 5, 10): (a) dimensionless journal orbit radius *e*/*c* vs speed parameter ω / ω_r; (b) transmissibility *T* vs speed parameter ω / ω_r (reproduced by permission of the ASME [51])

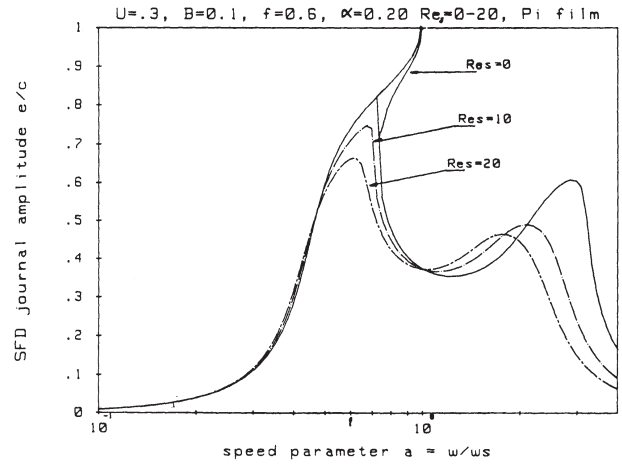

(a)

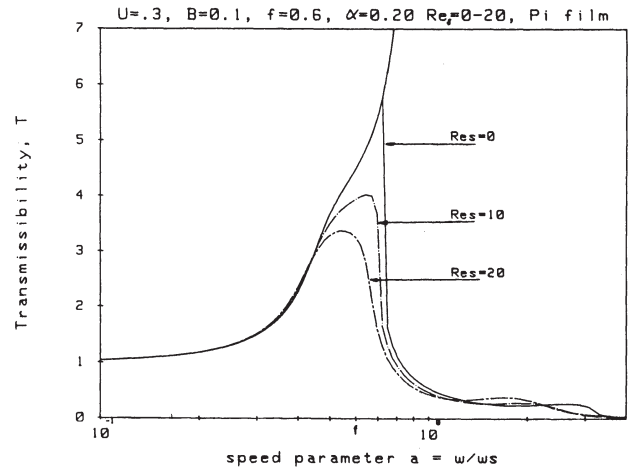

(b)

Figure 20. Theoretical frequency responses for the centralized, unbalanced flexible rotor, with unpressurized SFDs, in the absence of fluid inertia effects at the SFDs supports (Res = 0) and with inertia effects (Res = 5, 10): (a) dimensionless journal orbit radius *e*/*c* vs speed parameter ω / ω_s; (b) transmissibility *T* vs speed parameter ω / ω_s (reproduced by permission of the ASME [51])

Appreciable benefit due to the inertia effect was also observed for the flexible unbalanced rotor, under the hypothesis of cavitated film (see Figure 20(a); the Reynolds number Res in the figure was obtained from Re*, substituting the first pin-pin critical speed, here indicated as ω_s, in place of the whirling frequency ω), with the absence of jump, a considerable reduction in the whirling amplitudes and the forces transmitted to the frame, except for a narrow region downstream of the pin-pin critical speed (Figure 20(b)). Instead, no such evident benefits were observed for uncavitated film conditions. The inertia of the film only seemed to be responsible for a shift in the resonant speeds (this effect was present for cavitated conditions too). An attenuation of the amplitude of vibration was observed at the first critical speed, accompanied by an increase in the resonant peak at the second critical speed (Figure 21(a)). A similar influence of the inertia was observed with respect to the transmissibility (Figure 21(b)).

El-Shafei [52, 53] theoretically investigated the dynamic behavior of a flexible symmetrical unbalanced rotor with a single disk at mid-span, in the presence of fluid inertia effect in the SFDs placed at the end supports. The expression of the fluid film force, written with the use of the inertia coefficients, was obtained through the energy approximation method (see [1]). The πSBA and πLBA were alternatively adopted with the hypotheses of SCCOs of the journals and Re* up to 50. The solution of an algebraic polynomial equation, obtained from the equations of motion, made it possible to plot a series of curves that represented the amplitude-frequency response of the rotor. The data obtained with the SBA approximation (comparable, in the absence of fluid inertia, with the results reported by [4, 14]), showed a considerable reduction of the jump phenomena for low values of the unbalance parameter (< 0.1, 0.2) and suitably

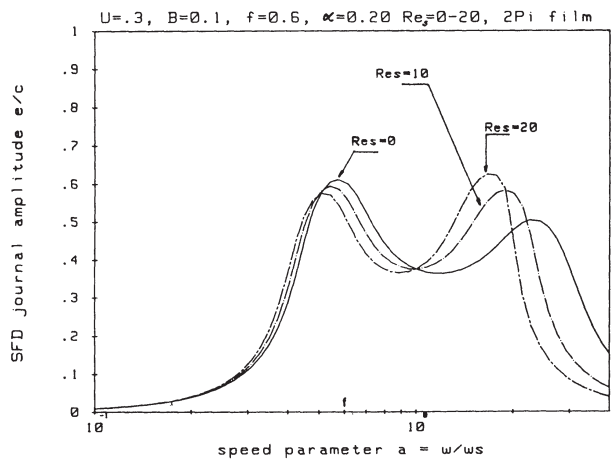

(a)

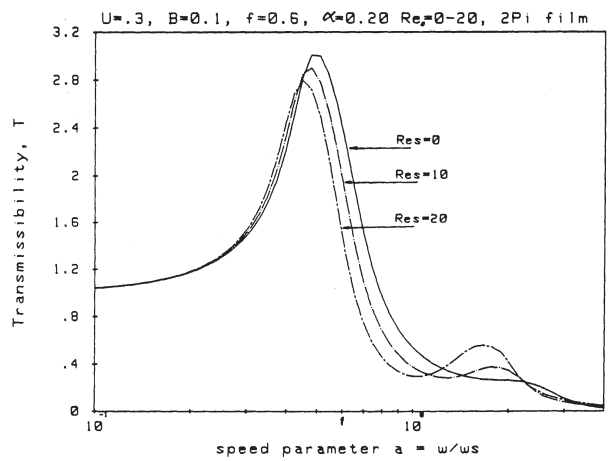

(b)

Figure 21. Theoretical frequency responses for the centralized, unbalanced flexible rotor, with pressurized SFDs, in the absence of fluid inertia effects at the SFDs supports (Res = 0) and with inertia effects (Res = 5, 10): (a) dimensionless journal orbit radius *e*/*c* vs speed parameter ω / ω_s; (b) transmissibility *T* vs speed parameter ω / ω_s (reproduced by permission of the ASME [51])

high values of the bearing parameter (≥ 0.1; this parameter was defined differently from [4, 14]), even though the latter condition made the transmissibility increase (in particular at speeds beyond the pin-pin c. s.). The ability of the inertia to reduce the importance of jump, as was observed in [51], was thus confirmed. Nevertheless, the same inertia effect in the SF supports placed at both ends of the rotor shaft, *gave rise to a second mode of vibration, with a worsening of the response in terms of vibration amplitude (measured at mid-span) and transmissibility*. The data relative to the LBA, after comparison with the corresponding results obtained with the short model, showed a better ability to reduce the amplitude of the precession motion, though higher values of the force transmitted to the frame resulted. A considerable reduction of the jump was also observed, even though further chances for the occurrence of the same phenomenon arose in connection with the second mode of vibration that was introduced by the inertia effect. Importantly, these results were assumed as a basis for the SFD improvement (section 4).

The influence of the fluid film cavitation on the dynamic behavior of the rotor was investigated, among others, in [54–58]. The cavitation typology (gaseous or vapor, etc.; see Part I), the extension of the cavitated zone, and the conditions for the lubricant supply, were all aspects deserving particular importance in the course of these studies. On the other hand, the importance of such aspects is witnessed by the recent and current investigation about the characteristics of SF in the presence of cavitation with entrained air, as reported at the end of Part I.

Feng and Hahn [57] investigated the dynamic response of an unbalanced, centralized, rigid rotor, focusing attention on the behavior of the cavitated lubricant film in the presence of dissolved air, regardless of seal effects. The amplitude-frequency responses, theoretically obtained in separate ways with four different models for the cavitated film, were compared. The above models represented two incompressible film models, the common π-film model and the *zero-pressure-truncation model*, respectively, and two compressible models, the *Hayward model* and the *Isbin model*. The last two models accounted for the presence of the air dissolved within the lubricant, for a given value of saturation pressure, in two different ways, so as to make the bi-phasic mixture constituting the film attain, respectively, a higher or lower viscosity with respect to that of pure oil. The theoretical data showed some differences between models in the amplitudes of the responses, together with a higher or lesser tendency to exhibit a bistable behavior (Figure 22(a)). Similarity in the responses could be respectively assessed between the Hayward and the zero-pressure-truncation models, on the one hand, and between the Isbin and the π-film models, on the other. Further comparison with the experimental amplitude-frequency response highlighted the better performance of the Hayward compressible model and the zero-pressure-truncation model with respect to those of the other two models (Figure 22(b)).

The analysis of Zeidan and Vance [56] noted, among other results, the fact that when cavitation occurs with a bi-phasic mixture of oil and air, the jump can arise with characteristics that are different from the cases characterized by vapor-cavitation or absence of cavitation. In the last two circumstances, the SFD behaves like a spring whose stiffness increases with ε, whereas, in the presence of air, the radial force may fall while increases because of the air compressibility. Consequently, during operations characterized by speed increase, the rotor response may be affected by jump-up instead of jump-down. The presence and role of the *softening spring* effect connected to the air entrainment was confirmed by the shift in the resonant peaks that manifested in the amplitude-speed response, might be inferred from comparing the run-up data relative to the pressurized film to those relative to unpressurized conditions.

The effect of the cavitating conditions within the squeeze film on rotor dynamics was also examined by Zhao et al. [58], who adopted an experimental, flexible, unsymmetrical rotor, that could be unbalanced in a static and coupled way. Of the two self-aligning ball bearings, supporting the rotor at

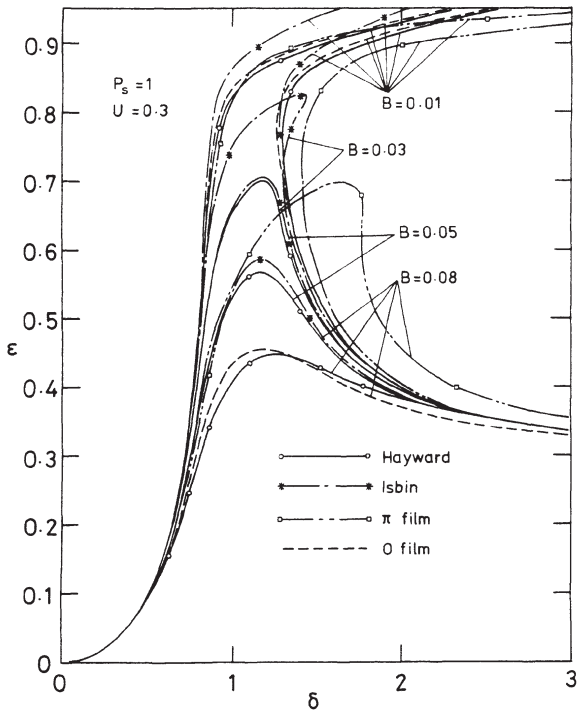

(a)

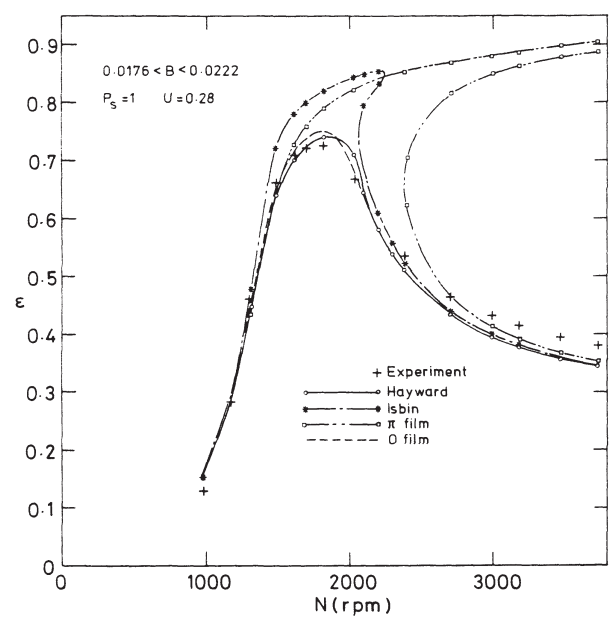

(b)

Figure 22. (a) Theoretical frequency responses (dimensionless journal orbit radius ε vs speed parameter δ) for the centralized, unbalanced flexible rotor, with different models of cavitation (unbalance parameter U = 0.3, different values of the bearing parameter B in the interval 0.01–0.08; P_s = 1 indicates lubricant saturated with air at atmospheric pressure; (b) comparison with the experimental response (dimensionless journal orbit radius ε vs rotor speed N) with U = 0.28, P_s =1 and 0.0176 < B < 0.0222 (reproduced by permission of the ASME [57])

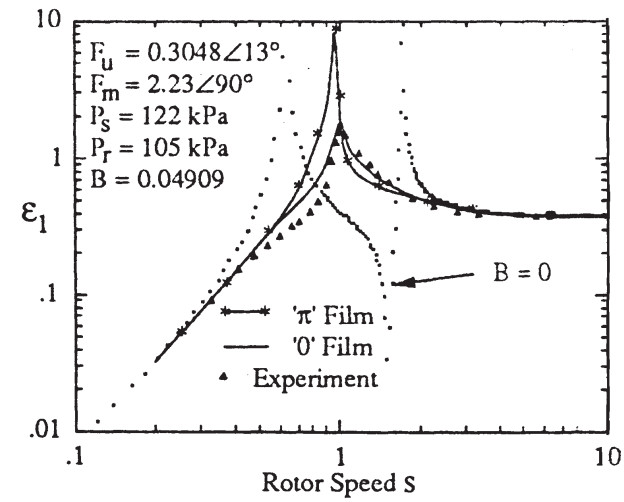

(a)

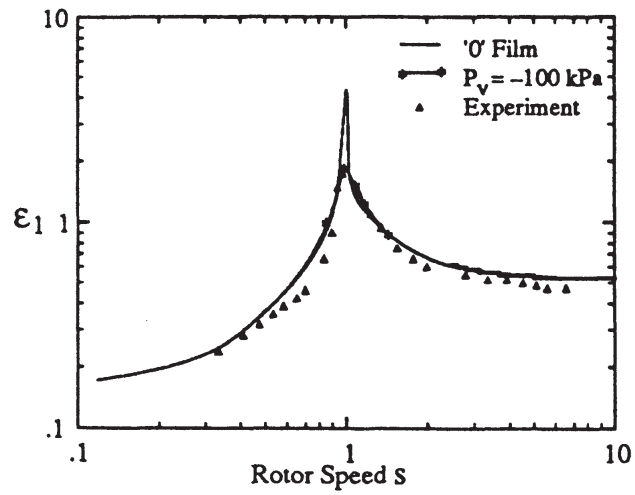

(b)

Figure 23. Comparison between experimental and theoretical responses (rotor middle eccentricity ratio ε_1 vs speed parameter s) for unbalanced flexible rotor (F_u and F_m are parameters for the static and couple unbalance, P_s, P_r and P_v indicate the supply, the return and the film rupture pressures): (a) concentric damper operation; (b) eccentric damper operation with dimensionless static eccentricity equal to ≈ 0.3 (reproduced by permission of the ASME [58])

both ends, one was equipped with SFD and retaining springs. The mass of the rotor was placed at mid-span (as a disk with specified mass moments of inertia) and at the SF support. Suitable values of the static eccentricity were set and the SF was provided with adjustable seals and fed at moderate values of the supply pressure. Both the experimental orbits and the amplitude-frequency responses were compared with their theoretical counterparts obtained according to the indications from Zhao [26] (the SBA and the TCM were adopted), where different cavitating models were taken into account. It was assumed that gaseous conditions (the film was assumed π-cavitated, with atmospheric value

of the absolute rupture pressure), vapor conditions (the film was also termed 0-cavitated, with null value of the absolute rupture pressure) or tensile stress conditions (characterized by negative values of the quasi-cavitation pressure) could arise within the fluid film during operation. The considerable effect on the dynamic behavior of the rotor turned out to depend on the actual conditions of the film, especially in the interval of speed near the first pin-pin critical speed. In this range, for concentric damper operations (i.e. in the absence of static eccentricity) and under the assigned dynamic unbalance conditions (moderate values), the film exhibited vapor cavitation or, at most, zones with tensile stress, and the authors noted the poor performance achieved by the π-film model (Figure 23(a)). In the presence of moderate static eccentricity too, the fluid film conditions were well predicted by the 0-cavitated model and the tensile stress model (especially near resonance, see Figure 23(b)). Instead, when the static eccentricity was given higher values with parallel increase in unbalance, gaseous cavitation arose along with unsteady motion, near the first pin-pin critical speed. A similar response was obtained for concentric operation at the highest unbalances. The interval of speed around the first pin-pin critical speed was affected by the sudden alternation of jump-up and jump-down that were due to the cyclic entrainment and flushing of air. The sudden increase in the orbit sizes, with the parallel rise of the journal towards the bearing centre, was explained by the authors in terms of the softening spring effect, due to air ingestion. This behavior, along with the presence of milky lubricant within the damper, justified the occurrence of the jump-up on run-up, which was unexpected on the basis of the hardening spring behavior congruent with the π-length model. In this respect the authors indicated the need to take account of the bi-phasic conditions within the fluid film (in accordance with the observations in [56]) and referred to the results of Feng [59]. The elimination of bistable behavior by increasing the supply pressure (the return pressure was checked too) was also experienced in the course of the tests.

Holmes and Dogan [54] obtained similar results for the cavitating conditions within the SF, as a consequence of varying the level of the supply pressure. The authors carried out a theoretical and experimental investigation with an unbalanced rigid rotor that was supported with a self-aligning ball bearing on the one end, and a SF support at the other end. An elastic suspension was mounted in series to the SF, interposed between the damper rig and the frame of the rotor. In this way, a simulation of the actual flexibility of the support structure, with particular reference to the operating conditions relative to an aeronautical engine, was achieved. A characteristic end-leakage factor (see [1]) was adopted in order to take into account the presence of seals, through a suitable combination of a short-bearing distribution of the pressure and a long-bearing one. During the experimental tests, the pressure recordings suggested that vapor cavitation, gaseous cavitation and tensile stress conditions could be respectively attained with subsequent increases in the supply pressure of the SF, before achieving full-film conditions that caused a consequent loss of the load-carrying capability. In this respect, the authors noted the role of the higher oil flow-rates in allowing the growth of a negative pressure within the film. The obtained data also showed that the increase in the supply pressure raised, near resonance, the amplitude of vibration of the unbalanced rotor relative to the supporting frame and the forces transmitted to the same structure, while leaving practically unchanged the size of the journal orbits within the damper ring. A series of tests addressed the effect of variations in the sealing gap on the damping and amplitude of vibration, for rigid support conditions. The effectiveness of the end-leakage factor adopted for the theoretical predictions was tested during this part of the investigation.

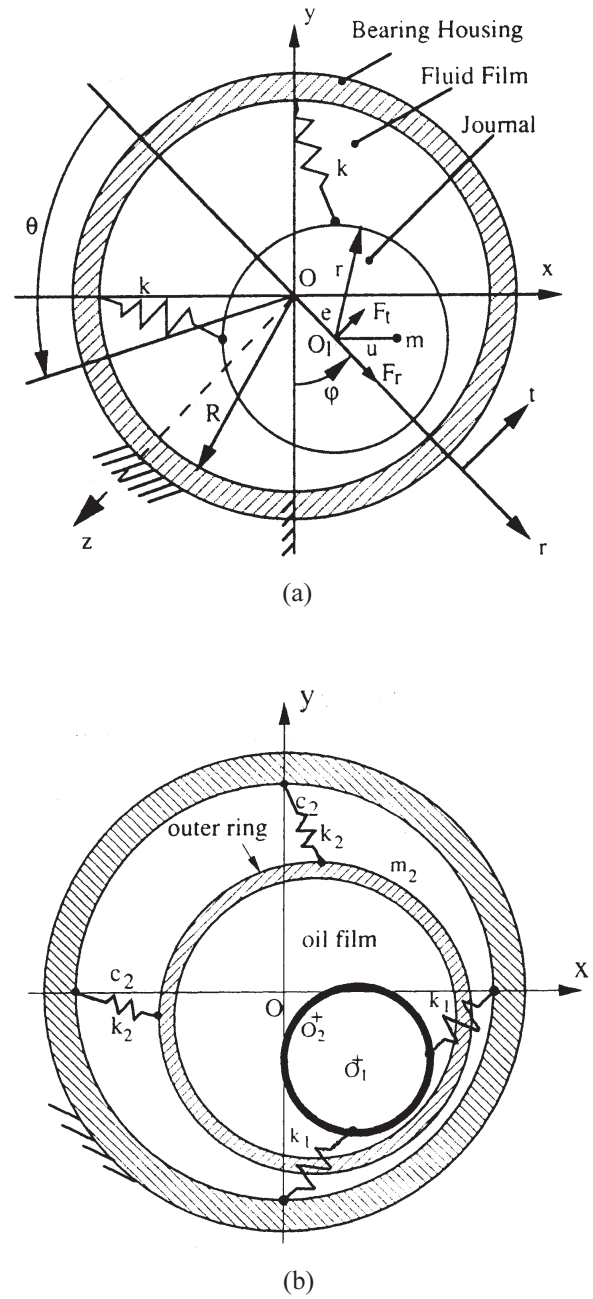

Figure 24 (a) Scheme of a typical SFD with retaining springs; (b) scheme of an improved SFD with support flexibility (O_1: journal center; O_2: bearing center; O: housing center) (reproduced by permission of the ASME [60])

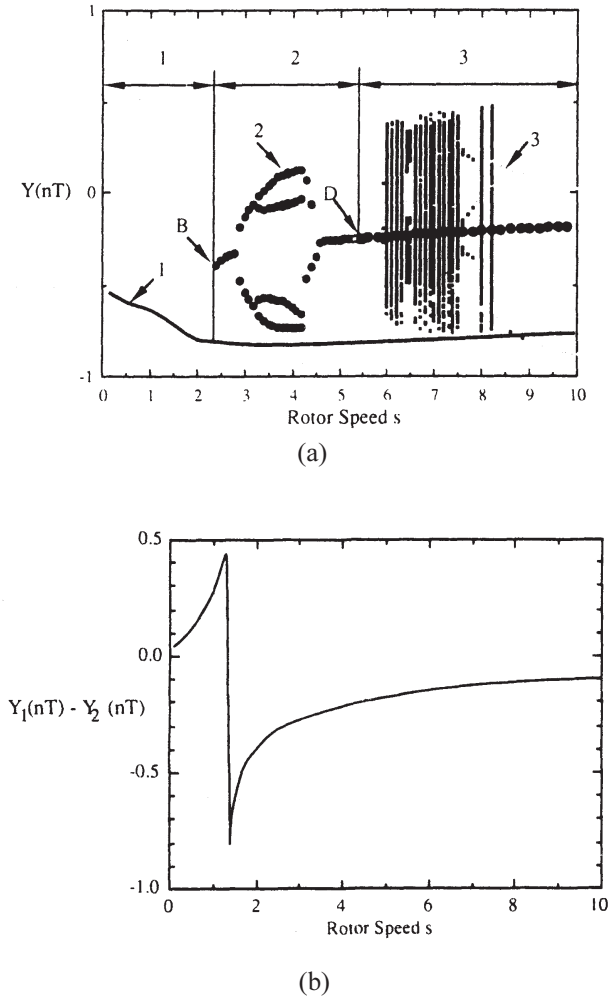

Figure 25. Bifurcation diagrams for a rigid rotor operating with conventional and improved supports, respectively (B_n = 0.1; U = 0.4; static eccentricity equal to – 0.6; the return points were collected with a time step equal to the period of rotation): (a) model with conventional supports; Y is the vertical displacement of the journal; (b) model with improved supports; $Y_1 - Y_2$ indicates the relative vertical displacement between the journal and the damper outer ring (reproduced by permission of the ASME [60])

The above analysis was extended by Holmes and Dede [55] who adopted the same system and examined the dependence of the dynamic response on the damping capacity of the fluid film, for different values of the supply pressure, the degree of sealing and the lubricant viscosity. In particular, examples were reported of sub-harmonic motion and jump-up. The jump-up arose due to run-up operation, after locking the elastic elements that supported the housing of the SFD, with operating conditions represented by low values of the oil viscosity and supply pressure, and rather high unbalance. In these circumstances, the onset of gaseous cavitation made the damper performance diminish (unlike [56, 58], the authors did not plunge into the mechanism that made the venting from atmosphere give rise to the jump phenomenon). On the basis of the reported theoretical and experimental results, Holmes and Dede considered the housing flexibility in series with the SFD critical and substantially negative.

The last aspect was also theoretically examined by Zhao and Hahn [60], who assumed the outer ring of the SFD elastically connected to the rigid frame (a typical scheme of SFD and the improved solution are respectively illustrated in Figure 24(a) and (b)). Such housing flexibility (refer to the springs marked with k_2 in Figure 24(b)), adopted in addition to the conventional arrangement with retainer springs (unlike [54, 55] where the lack of a centering suspension was assumed), was the peculiar characteristic of a theoretical model aimed at testing improvements in the SF support system. Concentric damper operation, eccentric damper operation and blade loss conditions were separately analyzed for a rigid rotor, comparing the theoretical response of the conventional arrangement with the corresponding response obtained with improved supports. After assumption of the πSBA, the amplitude-frequency responses were obtained by numerically integrating the equations of motion (unlike the concentric damper case that was treated by means of the TCM). The improved support solution, characterized by the housing flexibility, for the fixed set of parameters (the ratio between the mass of the rotor and that of the damper outer ring, and the ratio between the stiffnesses k_1 and k_2 illustrated in Figure 24(b), represented two additional parameters of the system) showed a good ability to prevent bistable conditions, sub-synchronous and nonsynchronous motions, thanks to quite a large range of quasi-linear behavior. An instance of such performance is illustrated in Figure 25(a) and (b) where the bifurcation diagrams theoretically obtained, respectively, with the conventional and improved supports, are compared. The benefits deriving from the housing flexibility are evident when observing in Figure 25(b) where the synchronous solution represented the only type of resulting motion. However, Zhao and Hahn noted the need for additional damping aimed at reducing the amplitude of rotor vibrations and damper flexible housing with respect to the ground at the first critical speed.

4. Improved or Novel SFDs, State-of-the-Art Research, Future Research Trends and Conclusions

The search for improvements in the damper bearing that distinguishes the above work of Zhao and Hahn broaches the subject of this concluding section of the review, that is focused on work aimed at SFD improvement, as it characterizes state-of-the-art research and future research trends in the field.

According to the surveyed investigations, our knowledge has been considerably advanced within the ambit of SFD arrangements that can be considered *conventional*, with particular regard to the fluid inertia effects, the geometry of grooves, the presence of seals, the cavitation of the film, etc., and their influence on those aspects leading to poor damper performance (as part of a rotor-support system), like jump phenomena, nonsynchronous motions and high levels of the transmitted forces.

Nevertheless, several discrepancies between theoretical and actual behavior suggest the need for further study, in order to assure reliable prediction of SFD performance in technical applications, and has addressed further research work. An example in this regard is represented by the studies on bubbly cavitation in open-end SFDs cited in sections 6.1 and 6.2 of Part I. The current situation has been briefly described by Vance et al. [61] with the following words: "…Twenty-five years of applied SFD research has failed to produce reliable design tools that can accurately predict the performance of any except the simplest geometry under laboratory conditions…".

On the other hand, the above scenario has fostered the recent search for new concept SFDs. Some pathways followed in this search can be indicated, as may be inferred from recent technical literature and industrial patents:

- recourse to unconventional geometries (involving the lubricated chamber, the elastic suspension, etc.),
- adoption of non-traditional fluids,
- recourse to the active control of the damper.

Use of unconventional geometries, within the ambit of a passive damper concept, is illustrated in the examples below.

Heshmat and Walton [62, 63] presented a *Multisqueeze Film Damper* (MSFD) where an inconel spiral thin foil was inserted as a single wrap within the clearance (suitably enlarged) of an SFD, with the ends attached to the damper journal and to the ring, respectively (Figures 26(a) and (b)). Besides representing, approximately, two squeeze film dampers in series (a higher number is possible with more wraps), the arrangement also achieved a centering function. The experimental data from tests carried out with a flexible rotor that could be normally or severely unbalanced made it possible to assess the effectiveness of the proposed damper in limiting the vibration amplitude and avoiding bistable behavior when the operating conditions are characterized by abusive loads (as resulting from partial or complete blade loss).

Zeidan et al. [64] and de Santiago, San Andres and Oliveras [65] proposed and tested an *Integral Squeeze Film Damper* (ISFD). The innovative design of the SFD allowed a substantial reduction in the axial dimensions with respect to the conventional arrangements. In fact, the retaining springs were machined integral with the body of the damper, as wire-EDM (electric discharge machines) webs connecting arcuate sector pads to the ring (Figures 27(a) and (b); in particular Figure 27(b) shows an "S" shaped ISFD in series with a tilting pad bearing). The squeeze film region was represented by the gap between the pads and the ring. Suitable machining, with appropriate offset given to the pads, made it possible to allow for the gravity load and center the journal. A series of tests with a rotor rig allowed identification of the viscous damping coefficients due to the ISFDs that exhibited an approximate linear increase with the amplitude of vibration (in some disagreement with the theoretical coefficients). A quasi-linear character of the system response could be generally recognized, with amplitudes of vibration at resonance that were linearly correlated to the unbalance and absence of shifts in the system resonances as a consequence of variations in the level of unbalance. The effectiveness of the ISFD was also noted in [64] with reference to the rig adopted by Murphy et al. [66], where the damper was used in the supports of a compulsator rotor (high damping capabilities were requested, because of the severe loads arising during the operation).

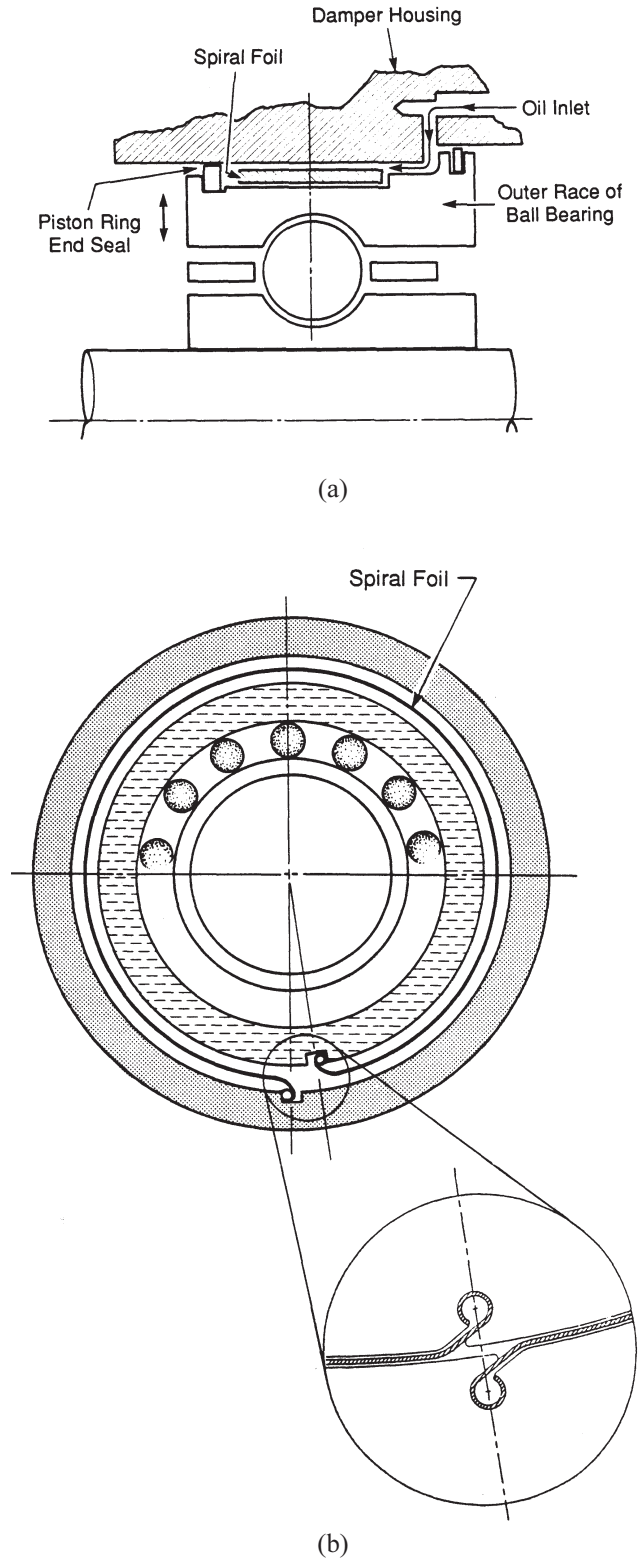

Figure 26. (a-b): spiral foil Multisqueeze Film Damper (single wrap) (reproduced by permission of the ASME [63])

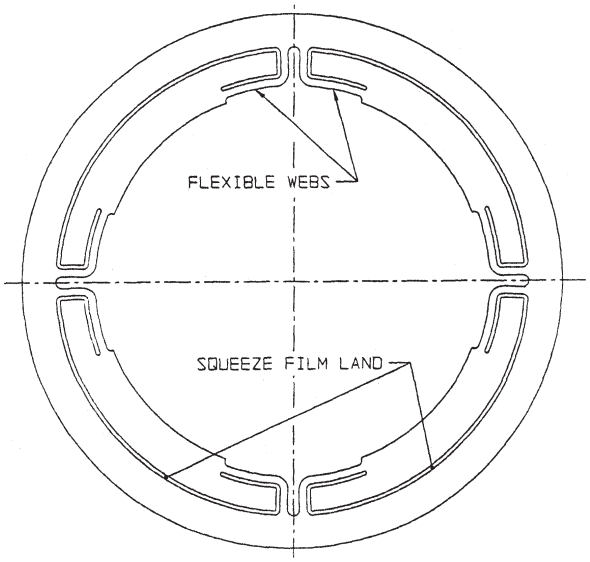

(a)

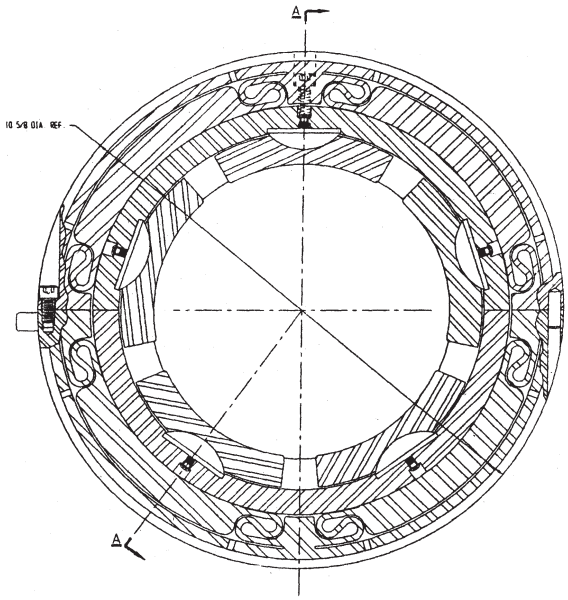

(b)

Figure 27. (a) Integral Squeeze Film Damper (ISFD); (b) ISFD in series with a tilting-pad bearing (courtesy of the Turbomachinery Laboratory [64])

A consistent saving of axial space was also achieved in the assembly proposed by a patent of the Asea Brown Boveri AG (inventor: Bättig) [67], where an SFD was coupled to an internal journal bearing, making use of a very compact centering element. This elastic suspension, arranged parallel to the damping film, consisted of an outer ring connected to an inner ring by means of intermediate bending rods (in a different configuration the bending rods were replaced by segments that constituted a characteristic cardan ring; the EDM was a possible way, as an alternative to precision casting, to manufacture the centering element). The use of a compact centering spring was also a characteristic of the SFD patented by the Ishikawajima-Harima J. K. K. (inventors: Soichiro Une et al.) [68]. A series of concentricity spring means, placed midway along the axial length of the damper, were realized by press-machining a thin stainless steel sheet and then bending it into a cylindrical shape so as to appear like a whole ring, of suitable axial dimension, made up of a number of arcuate segments. Under many aspects, the device resembled the corrugated bump foil of a foil journal bearing [69, 70].

An unconventional geometry for the lubricated chamber of the SFD was proposed by a patent of the General Electric Company (inventor: Dede, M. M.) [71] where, in place of a single cylindrical wall, the housing of the SFD adopted a number (two at least) of nonconcentric cylindrical portions. These portions could be axially spaced along the axis of the damper or, alternatively, overlapped so as to give the chamber a multi-lobe configuration. The presence of different nonconcentric cylindrical segments of the lubricated annulus was claimed as a characteristic that is apt to reduce bistable behavior, to contain the amplitude of vibration at resonance, and to increase the radial force, so as to make the presence of retaining springs unnecessary.

A variable geometry with an active control logic was implemented by El-Shafei and co-workers on the HSFD (Hybrid SFD) [72–77]. Experience with rotors supported on conventional SFDs made the author infer that rotor operation could be optimized if the damper is operated as a *short* one in some ranges of speed and as a *long* one in other ranges (see [52, 53, 73, 74] and section 3.5). The former configuration is more effective in limiting the transmission of force to the support while the latter configuration, because of the high damping capacity, allows a better reduction of the amplitude response of the rotor. As a consequence, the long damper configuration is recommended during run-up and coast down, thanks to its ability to attenuate the vibration peaks and jump phenomena. Conversely, the short damper configuration is beneficial at operating speeds above resonance, where it is more effective than the long damper in reducing the force at supports. Furthermore and importantly, it avoids the possible second critical speed due to fluid inertia that affects the operation with long dampers. On this basis, El-Shafei proposed a device that could *switch* the operation of the damper between the short and long configurations, by controlling the sealing of the damper through the intervention or the removal of movable lateral seals. This solution has been a driving force behind implementing *active vibration control* of rotors capable of tackling both the crossing of critical speeds and the sudden transients such as those owing to blade loss [75–77].

In this regard, the investigations of Burrows et al. [78] and Adams and Zahloul [79] should be mentioned, as they are early indications about the use of ASFDs (*Active* SFDs). Both studies suggested the control of pressure as a means of acting on damper and rotor performance (the latter work dealt with hydrostatic SFDs). Burrows and co-workers highlighted the advantages of this solution, as a technique

that represented a promising alternative to the use of *magnetic bearings* for the control of rotors. Indeed, according to El-Shafei and El-Hakim [77], the use of enhanced ASFDs in place of magnetic bearings is still a very topical issue.

Various other techniques have been investigated or proposed for the implementation of ASFDs. In a patent of Mitsubishi Heavy Industries Ltd., the inventors (Hamanaka Sachiko et al.) [80] presented a device that gives rise to a simple variation of the axial length of the squeeze area. Mu et al. [81] made recourse to a movable conical damper ring. Yunhua et al. [82] proposed a hybrid SFD, capable of combining hydrostatic and hydrodynamic modes, thanks to electrohydraulic controllable orifices with PZT actuators.

The replacement of common lubricants with non-traditional damping fluids has lately become a significant prospect, with particular regard to the capability of active control. On the one hand, basic research into non-Newtonian squeeze films has been continued (some instances are given in [83–85]). On the other hand, a specific class of fluids, represented by the ER (electrorheological) fluids and MR (magnetorheological) fluids, has received increasing interest for use with dampers and particularly with SFDs. ER fluids (also called electroviscous fluids) and MR fluids [86–89] exhibit the remarkable feature of varying their yield shear stress (through the assumption of a non-Newtonian character, i.e. that of a Bingham fluid) with the intensity of an applied electric or magnetic field, respectively (very fast changes can be obtained). These properties have been well known for decades [90] but only in recent years has the availability of low-cost fluids with improved characteristics given an appreciable impetus to industrial applications. Leaving aside a very broad series of theoretical papers, laboratory tests and industrial patents regarding the field of ER/MR-fluid based damping devices for vibration suppression (and relative control) [91], the application to SFDs has been investigated at some degree even though this technique is still at an early stage. Despite the theoretical attention shown by recent papers [92–96], commercial implementation and practical use of ER-based SFD seem quite premature, although some industrial patents can be found [97]. Yet, in a recent work [98], actually focused on a disk type ER damper (the damping fluid works in a *shear-mode* rather than *squeeze-mode* [99]), and in a companion paper about comparative tests regarding different systems for actively controlled damping in aircraft engines [61], Vance et al. express considerable scepticism about the capabilities offered by the present development of ER dampers for turbomachinery application. With reference to tests made with the disk type ER damper, the investigators reported the shortcomings connected with the use of ER-fluids, like electrical arcing and the commercial unavailability of proper ER fluids, going so far as to explicitly claim the current inadequacy of this technique, especially when compared with the use of passive SFDs.

With respect to ER fluids, MR fluids exhibit more favorable characteristics. Yield stresses approximately two magnitudes greater than in the case of ER fluids can be obtained. Furthermore, MR fluids show better tolerance of impurities, better stability over a wide temperature range and, importantly, require low voltage power supplies (0 ÷ 50 V), against the very high voltage power supplies (up to 5,000 V) required by ER fluids. Examples of investigations with MR fluid-based SFDs are given in [100–104]. A rotordynamic evaluation of an on-off control of the MR-SFD was carried out in [102], with adoption of a flexible unbalanced rotor. The bearing damper was mounted at one end of the rotor and was equipped with centralizing springs. The active control was capable of tackling the first two critical speeds of the rotor. In particular, the following factors were taken into account: the effect of different applied voltages (0 ÷ 10 V), the incidence of different fluid compositions, the possible influence of the magnetic pull force between the journal and the damper, and the influence of the residual magnetic field and initial fluid viscosity on the sediment process within the MR fluid.

It seems of some interest to conclude the present review by discussing a recent example of *unconventional* applications of SFDs. This is the case of the SFD&VG (Squeeze Film Damper and Vibration Generator) [105], where an actively controlled SFD is suitably adopted for the industrial drilling of deep holes. The vibratory component needed for such drilling is guaranteed, fairly inexpensively, by this special SFD, whose variable geometry allows the generation of periodic forces.

The previous sections of the paper provide a necessarily incomplete survey of the theoretical and experimental studies carried out on the SFD. Nevertheless, the above-mentioned review makes it possible to predict some considerable amount of investigation in this field: future enquiries are likely to focus on the application of active control techniques and the use of smart fluids (i.e ER and MR fluids) and materials, together with the need for improved theoretical knowledge, capable of ensuring reliable design tools in the use of traditional passive SFDs, especially in the case of advanced geometries and arrangements.

References

[1] Della Pietra, L., and Adiletta, G., 2002, "The Squeeze Film Damper over Four Decades of Investigations. Part I: Characteristics and Operating Features," *The Shock and Vibration Digest*, Vol. 34.

[2] Hahn, E. J., 1979, "Stability and Unbalance Response of Centrally Preloaded Rotors Mounted in Journal and Squeeze Film Bearings," *ASME J. Lubrication Technology*, Vol. 101, 120-128.

[3] Gunter, E. J., 1966, "Dynamic Stability of Rotor-Bearing Systems," NASA SP-113 (N67-11942), National Technical Information Service, Washington.

[4] White, D. C., 1970, "Squeeze Film Journal Bearings," Ph.D. Dissertation, Cambridge University.

[5] Hahn, E. J., and Simandiri, S., 1974, "Squeeze Film Mounts for Vibration Attenuation in Rigid Rotors," *Proc. Noise, Shock & Vibration Conference*, Monash Univ., Melbourne.

[6] Mohan, S., and Hahn, E. J., 1974, "Design of Squeeze Film Damper Supports for Rigid Rotors," *ASME J. Engineering for Industry*, Vol. 96, 976-982.

[7] Taylor, D. L., and Kumar, K., 1983, "Closed-Form, Steady-State Solution for the Unbalance Response of a Rigid Rotor in Squeeze Film Damper," *ASME J. Engineering for Power*, Vol. 105, 551-559.

[8] Hahn, E. J., 1980, "Squeeze Film Bearings as Vibration Isolators for Unbalanced Rigid Rotors," *ASLE Transactions*, Vol. 24(2), 239-246.

[9] Taylor, D. L., and Kumar, K., 1980, "Nonlinear Response of Short Squeeze Film Dampers," *ASME J. Lubrication Technology*, Vol. 102, 51-58.

[10] Simandiri, S., and Hahn, E. J., 1979, "Experimental Evaluation of the Predicted Behaviour of Squeeze Film Bearing Supported Rigid Rotors," *ImechE, J. Mechanical Engineering Science*, Vol. 21, 6, 439-451.

[11] Simandiri, S., and Hahn, E. J., 1976, "Effect of Pressurization on the Vibration Isolation Capability of Squeeze Film Bearings," *ASME J. Engineering for Industry*, Vol. 98, Series B, N.1, 109-117.

[12] Rabinowitz, M. D., and Hahn, E. J., 1977, "Stability of Squeeze-Film-Damper Supported Flexible Rotors," *ASME J. Engineering for Power*, Vol. 99, 545-551.

[13] McLean, L. J., and Hahn, E. J., 1985, "Stability of Squeeze Film Damped Multi-Mass Flexible Rotor Bearing Systems," *ASME J. Tribology*, Vol. 107, 402-410.

[14] Rabinowitz, M. D., and Hahn, E. J., 1977, "Steady-State Performance of Squeeze Film Damper Supported Flexible Rotors," *ASME J. Engineering for Power*, Vol. 99, 552-558.

[15] Cunningham, R. E., Fleming, D. P., and Gunter, E. J., 1975, "Design of a Squeeze-Film Damper for a Multi-Mass Flexible Rotor," *ASME J. Engineering for Industry*, Vol. 97, 1383-1389.

[16] McLean, L. J., and Hahn, E. J., 1983, "Unbalance Behaviour of Squeeze Film Damped Multi-Mass Flexible Rotor Bearing Systems," *ASME J. Lubrication Technology*, Vol. 105, 22-28.

[17] Hahn, E. J., and Chen, P.Y.P., 1994, "Harmonic Balance Analysis of General Squeeze Film Damped Multidegree-of-Freedom Rotor Bearing Systems," *ASME J. Tribology*, Vol. 116, 499-507.

[18] Zhao, J. Y., Linnet, I. W., and McLean, L. J., 1994, "Stability and Bifurcation of Unbalanced Response of a Squeeze Film Damped Flexible Rotor," *ASME J. Tribology*, Vol. 116, 361-368.

[19] Kirk, R. G., and Gunter, E. J., 1972, "The Effect of Support Flexibility and Damping on the Synchronous Response of a Single Mass Rotor," *ASME J. Engineering for Industry*, Vol. 94, 221-232.

[20] Gunter, E. J., 1966, "Dynamic Stability of Rotor-Bearing Systems," NASA SP-113 (N67-11942), National Technical Information Service, Washington.

[21] Gunter, E. J., Barrett, L. E., and Allaire, P. E., 1976, "Stabilization of Turbomachinery with Squeeze Film Dampers – Theory and Applications," *IMechE*, C233/76, 291-300.

[22] Cunningham, R. E., 1978, "Steady-state unbalance response of a three-disk flexible rotor on flexible, damped supports," *ASME J. Mechanical Design*, Vol. 100, 563-573.

[23] Samoilenko, A. M., and Ronto, N. I., 1979, *Numerical-Analytic Methods of Investigating Periodic Solutions*, Mir Publishers, Moscow.

[24] Nataraj, C., and Nelson, H. D., 1989, "Periodic Solutions in Rotor Dynamic Systems with Nonlinear Supports: a General Approach," *ASME J. Vibr., Acoustics, Stress and Reliability in Design*, Vol. 111, 187-193.

[25] Seydel., R., 1988, *From Equilibrium to Chaos: Practical Bifurcation and Stability Analysis*, Elsevier Science Publishing.

[26] Zhao, J. Y., 1993, "Theoretical and Experimental Investigations of Eccentric Damper Operation of Squeeze Film Dampers," Ph.D. Thesis, Australian Defence Force Academy, University of New South Wales, Australia.

[27] Hsu, C. S., 1972, "Impulsive Parametric Excitation: Theory," *ASME J. Applied Mechanics*, Vol. 39, 551-558.

[28] Vance, J. M., 1988, *Rotordynamics of Turbomachinery*, Wiley & Sons.

[29] Li Xuehai, and Taylor, D. L., 1987, "Nonsyncronous Motion of Squeeze Film Damper Systems," *ASME J. Tribology*, Vol. 109, 169-176.

[30] Cooper, S., 1963, "Preliminary Investigation of Oil Films for Control of Vibration", Proc. Lubrication and Wear Convention, *Inst. Mech. Engin.*, 305-315.

[31] Gunter, E. J., Barrett, L. E., Allaire, P. E., 1977, "Design of Non Linear Squeeze-Film Dampers for Aircraft Engines," *ASME J. Lubrication Technology*, Vol. 99, 57-64.

[32] Pan, C.H.T., and Tonnesen, J., 1978, "Eccentric Operation of the Squeeze-Film Damper," *ASME J. Lubrication Technology*, Vol. 100, 369-378.

[33] Cookson, R. A., and Kossa, S. S., 1979, "The Effectiveness of Squeeze- Film Damper Bearings Supporting Rigid Rotors without a Centralising Spring," *Int. J. Mech. Sci.*, Vol. 21, 639-650.

[34] Holmes, R., and Sykes, J.E.H., 1989, "Large-Amplitude Vibrations in Rotor Assemblies," *J. Sound and Vibration*, Vol. 133(2), 337-351.

[35] Zhao, J. Y., and Hahn, E. J., 1993, "Subharmonic, Quasi-Periodic and Chaotic Motions of a Rigid Rotor Supported by an Eccentric Squeeze Film Damper," *IMechE, Proc Inst Mech Engrs*, *Part C: J. Mechanical Engineering Science*, Vol. 207, 383-392.

[36] Shiau, T. N., Hwang, J. L., and Chang, Y. B., 1993, "A Study on Stability and Response of a Nonlinear Rotor System with Mass Unbalance and Side Load," *ASME J. Engineering Gas Turbines and Power*, Vol. 115, 218-226.

[37] Zhao, J. Y., Linnet, I. W., and McLean, L. J., 1994, "Subharmonic and Quasi-Periodic Motions of an Ecccentric Squeeze Film Damper-Mounted Rigid Rotor," *ASME J. Vibration and Acoustics*, Vol. 116, 357-363.

[38] Hwang, J. L., and Shiau, T. N., 1991, "An Application of the Generalized Polynomial Expansion Method to Nonlinear Rotor Bearing Systems," *ASME J. Vibration and Acoustics*, Vol. 113, 299-308.

[39] Cookson, R. A., and Kossa, S. S., 1981, "The Vibration Isolating Properties of Uncentralized Squeeze-Film Damper Bearings Supporting a Flexible Rotor", *ASME J. Engineering for Power*, Vol. 103, 781-787.

[40] Shiau, T., and Jean A., 1990, "Prediction and Periodic Response of Flexible Mechanical Systems with Nonlinear Characteristics," *ASME J. Vibration and Acoustics*, Vol. 112, 501-507.

[41] Saito, S., 1994, "Nonlinear vibration of Horizontal Jeffcott Rotors Supported by Oil Film Damper Bearings Having No Centering Springs (Calculation of Nonlinear Imbalance Response and Forced Damper Natural Frequency)," *JSME Int. J., Series C*, Vol. 37, N. 1, 55-60.

[42] Zhang, J. Z., Xu Q., and Zheng T., 1998, "Stability and Bifurcation of a Rotor Fluid Film Bearing System with Squeeze Film Damper," *ASME J. Vibration and Acoustics*, Vol. 120, 1003-1006.

[43] Botman, M., Samaha, M. A., 1982, "Experiments on the Dynamic Behaviour of a Supercritical Rotor," *ASME J. Mechanical Design*, Vol. 104, 364-369.

[44] McLean, L. J., and Hahn, E. J., 1983, "A Design Study of Gyroscopic Effects on the Critical Speed of Flexibly Mounted Rotors," Kensington, University of South Wales, 1983/AM/3.

[45] Chu, F., and Holmes, R., 1998, "The Effect of Squeeze Film Damper Parameters on the Unbalancce Response and Stability of a Flexible Rotor," *ASME J. Engineering for Gas Turbines and Power*, Vol. 120, 140-148.

[46] Greenhill, L. M., and Nelson, H. D., 1981, "Iterative Determination of Squeeze Film Damper Eccentricity for Flexible Rotor Systems," *ASME J. Mechanical Design*, Paper 81-DET-87, 1-5.

[47] Shiau, T., and Hwang J. L., 1993, "Generalized Polynomial Expansion Method for the Dynamic Analysis of Rotor-Bearing Systems," *ASME J. Engineering for Gas Turbines and Power*, Vol. 115, 209-217.

[48] Kanki, H., Kaneko, Y., Kurosawa, M., and Yamamoto, T., 1998, "Prevention of Low-Frequency Vibration of High-Capacity Steam Turbine Units by Squeeze-Film Damper," *ASME J. Engineering for Gas Turbines and Power*, Vol. 120, 391-396.

[49] San Andrés, L., and Lubell, D., 1998, "Imbalance Response of a Test Rotor Supported on Squeeze Film Dampers," *ASME J. Engineering for Gas Turbines and Power*, Vol. 120, 397-404.

[50] Szeri, A. Z., Raimondi, A. A., Giron-Duarte A., 1983, "Linear Force Coefficients for Squeeze Film Dampers," *ASME J. Lubrication Technology*, Vol. 105, 326-334.

[51] San Andres L. A., and Vance J. M., 1988, "Effects of Fluid Inertia on the Performance of Squeeze-Film Damper Supported Rotors," *ASME J. Engineering for Gas Turbines and Power*, Vol. 110, 51-57.

[52] El-Shafei, A., 1990, "Unbalance Response of a Jeffcott Rotor Incorporating Short Squeeze Film Dampers," *ASME J. Engineering for Gas Turbines and Power*, Vol. 112, 445-453.

[53] El-Shafei, A., 1991, "Unbalance Response of a Jeffcott Rotor Incorporating Long Squeeze Film Dampers," *ASME J. Vibration and Acoustics*, Vol. 113, 85-94.

[54] Holmes, R., and Dogan, M., 1985, "The Performance of a Sealed Squeeze Film Bearings in a Flexible Support Structure," *IMechE, Proc. Inst. Mech. Engrs.*, Vol. 199, N. C1, 1-9.

[55] Holmes, R., and Dede, M. M., 1989, "Non Linear Phenomena in Aero-Engine Rotor Vibration," *IMechE Proc. Inst. Mech. Engrs, Part A: J.Power Engineering*, Vol. 203, 25-34.

[56] Zeidan, F., and Vance, J., 1990, "Cavitation and Air Entrainment Effects on the Response of Squeeze Film Supported Rotors," *ASME J. of Tribology*, Vol. 112, 347-353.

[57] Feng, N. S., and Hahn, E. J., 1987, "Effects of Gas Entrainment on Squeeze Film Damper Performance," *ASME J. Tribology*, Vol. 109, 149-154.

[58] Zhao, J. Y., Linnet, I. W., and McLean, L. J., 1998, "Unbalance Response of a Flexible Rotor Supported by a Squeeze Film Damper," *ASME J. Vibration and Acoustics*, Vol. 120, 32-38.

[59] Feng, N. S., 1988, "Cavitation Effects on Squeeze Film Damper Performance," PhD Thesis, The University of New South Wales, Australia.

[60] Zhao, J. Y., and Hahn, E. J., 1995, "Eccentric Operation and Blade-Loss Simulation of a Rigid Rotor Supported by an Improved Squeeze Film Damper," *ASME J. Tribology*, Vol. 117, 490-497.

[61] Vance, J. M., Ying, D., and Nikolajsen, J. L., 2000, "Actively Controlled Bearing Dampers for Aircraft Engine Applications", *ASME J. Engineering for Gas Turbines and Power*, Vol. 122, 466-472.

[62] Heshmat, H., and Walton, J., 1990, "Advanced Multisqueeze Film Dampers for Rotor Vibration Control," *ASME/STLE 1990 Tribology Conference Preprint, No. 90-TC-3E-1.*

[63] Walton II, J. F., and Heshmat, H., 1993, "Rotordynamic Evaluation of an Advanced Multisqueeze Film Damper - Imbalance Response and Blade Loss Simulation," *ASME J. Engineering for Gas Turbines and Power*, Vol. 115, 347-352.

[64] Zeidan, F. , San Andrés L. A., and Vance, J. M., 1996, "Design and Application of Squeeze Film Dampers in Rotating Machinery," Proceedings of the Twenty-Fifth Turbomachinery Symposium, Turbomachinery Laboratory, Texas A&M University, College Station, TX, 169-188.

[65] de Santiago, O., San Andrés, L., and Oliveras, J., 1999, "Imbalance Response of a Rotor Supported on Open-Ends Integral Squeeze Film Dampers," *ASME J. Engineering for Gas Turbines and Power*, Vol. 121, 718-721.

[66] Murphy, B. T., Manifold, S. M., and Kitzmiller, J.R., 1997, "Compulsator Rotordynamics and Suspension Design," *IEEE Transactions on Magnetics Mag*, Vol. 33(1), 474-479.

[67] US Patent 6,155,720, Dec. 5, 2000, "Journal Bearing," Inventor: Bättig J., Assignee: Asea Brown Boveri AG.

[68] JP Patent JP11002240 (equiv. US 5,988,888), Dec. 16, 1998, "Squeeze Film Damper Bearing," Inventors: Soichiro Une et al., Assignee: Ishikawajima-Harima Jukogyo Kabushiki Kaisha.

[69] US Patent 5,902,049, May 11, 1999, "High Load Capacity Compliant Foil Hydrodynamic Journal Bearing," Inventor: Heshmat, H., Assignee: Mohawk Innovative Technology, Inc.

[70] Heshmat, H., 1994, "Advancements in the Performance of Aerodynamics Foil Journal Bearings: high Speed and High Load Capability," *ASME J. Tribology*, Vol. 116, 287-295.

[71] US Patent 6,135,639, Oct. 24, 2000, "Fixed Arc Squeeze Film Bearing Damper," Inventor: Dede, M. M., Assignee: General Electric Company.

[72] US Patent 5,058,452, Oct. 22, 1991, "Hybrid Squeeze Film Damper for Active Control of Rotors," Inventor: El-Shafei, A., Assignee: University of South Florida.

[73] El-Shafei, A., 1993, "Experimental and Analytical Investigation of Hybrid Squeeze Film Dampers," *ASME J. Engineering for Gas Turbines and Power*, Vol. 115, 353-359.

[74] El-Shafei, A., 1988, "Dynamics of Rotors Incorporating Squeeze Film Dampers," Ph.D. Thesis, Massachusetts Institute of Technology, Cambridge, MA.

[75] El-Shafei, A., and El-Hakim, M., 1995, "Development of a Test Rig and Experimental Verification of the Performance of HSFDs for Active Control of Rotors," *ASME Paper No. 95-GT-256*.

[76] Hathout, J. P., and El-Shafei, A., 1997, "PI Control of HSFDs for Active Control of Rotor-Bearing Systems," *ASME J. Engineering for Gas Turbines and Power*, Vol. 119, 658-667.

[77] El-Shafei, A., and El-Hakim, M., 2000, "Experimental Investigation of Adaptive Control Applied to HSFD Supported Rotors," *ASME J. Engineering for Gas Turbines and Power*, Vol. 122, 685-692.

[78] Burrows, C. R., Sahinkaya, M. N., and Turkay, O. S., 1983, "An Adaptive Squeeze-Film Bearing," *ASME Paper N. 83-Lub-23*.

[79] Adams, M. L., and Zahloul, H., 1987, "Attenuation of Rotor Vibration Using Controlled-Pressure Hydrostatic Squeeze-Film Dampers," presented at the 11th Biennial Asme Vibration Conference, Boston, MA, September 1987.

[80] JP Patent JP11159126, Jun. 15, 1999, "Squeeze Film Damper Bearing," Inventors: Hamanaka Sachiko et al., Assignee: Mitsubishi Heavy Industries, Ltd.

[81] Mu, C., Darling, J., and Burrows, R.,1991, "An Appraisal of a Proposed Active Squeeze Film Damper," *ASME J. Tribology*, Vol. 113, 750-754.

[82] Yunhua, L, Zhanlin, W., and Jieli, C., 1999, "Solution for Pressure Distribution in Squeeze Film Damper with Electrohydraulic Active Control," *Chinese Journal of Mechanical Engineering*, Vol. 12(1).

[83] Hashimoto, H., 1994, "Viscoelastic Squeeze Film Characteristics With Inertia Effects Between Two Parallel Circular Plates Under Sinusoidal Motion," *ASME J. Tribology*, Vol. 116, 161-166.

[84] Lin, J-R., 1998, "Squeeze Film Characteristics of Finite Journal Bearings: Couple Stress Fluid Model," *Tribology Internat.*, Vol. 31, 53-58.

[85] Lin, J-R., Yang, C-B, and Lu, R-F, 2001, "Effects of couple stresses in the cyclic squeeze films of finite partial journal bearings," *Tribology Internat.*, Vol. 34, 119-125.

[86] US Patent 5,498,363, Mar. 12, 1996, "Electrorheological Fluid," Inventors: Ryoichi Kishi et al., Assignee: Agency of Industrial Science and Technology, Tokyo, Japan.

[87] US Patent 5,910,269, Jun. 8, 1999, "Electrorheological Fluid Composition Including Hydrocarbon Compound Having at Least One Unsaturated Bound," Inventors: Satoru Ono et al., Assignee: Nippon Shokubai Co., Ltd., Osaka, Japan.

[88] US Patent 5,985,168, Nov. 16, 1999, "Magnetorheological Fluid," Inventor: Phule, P. P., Assignee: University of Pittsburgh of the Commonwealth System of Higher Education, Pittsburgh, Pa.

[89] "*Electro-Rheological Fluids and Magneto-Rheological Suspensions*", *Proceedings of the 7th International Conference*, Honolulu, Hawaii 9–23 July 1999, edited by R. Tao, World Scientific, Singapore, London, 2000.

[90] Winslow, W. H., 1949, "Induced Fibration Suspensions," *J. Applied Physics*, Vol. 20, 1137-1140.

[91] Sims, N. D., Stanway, R., and Johnson, A. R., 1999, "Vibration Control Using Smart Fluids: a State-of-the-Art Review," *Shock and Vibration Digest*, Vol. 31, 195-204.

[92] Morishita, S., and Mitsui, J., 1991, "Controllable Squeeze Film Damper: An Application of Electro-Rheological Fluid," *Rotating Machinery and Vehicle Dynamics*, Vol. 35, 257-262.

[93] Dimarogonas, A. and Kollias, A., 1992, "Electrorheological Fluid-Controlled "Smart" Journal Bearings," *STLE Tribology Transactions*, Vol. 35, 611-618.

[94] Jung, S. Y., and Choi, S.-B., 1995, "Analysis of a Short Squeeze Film Damper Operating with Electrorheological Fluid," *STLE Tribology Transactions*, Vol. 38, 857-862.

[95] Pecheux, B., Bonneau, O., and Frêne, J., 1997, "Investigation about Electro-Rheological Squeeze Film Damper Applied to Active Control of Rotor Dynamic," *International J. Rotating Machinery*, Vol. 3, 53-60.

[96] Kim, C.-H., Lee, N.-S., Lee, Y.-B., and Choi, D.-H., 1998, "Vibration control of a Pressurized, Sealed, Electrorheological Fluid Squeeze Film Damper Supported Rotor," 7th International Symposium on transport Phenomena and Dynamics of Rotating Machinery, ISROMAC 7, Honolulu, Hawaii, Vol. A, 238-247.

[97] JP Patent JP2000145768, May 26, 2000, "Squeeze Film Damper Bearing," Inventors: Murai Yoichi et al., Assignee: Hitachi, Ltd.

[98] Vance, J. M., and Ying, D., 2000, "Experimental Measurements of Actively Controlled Bearing Damping With an Electrorheological Fluid," *ASME J. Engineering for Gas Turbines and Power*, Vol. 122, 337-344.

[99] Nikolajsen, J. L., and Hoque, M. S., 1988, "An Electroviscous Damper," "*Rotordynamic Instability Problems in High-Performance Turbomachinery,*" NASA CP 3026, 133-141.

[100] M. R. Jolly et al., 1996, "Controllable Squeeze Film Damping Using Magnetorheological Fluid," 5th International Conference on New Actuators, ACTUATOR 96, Jun. 26-28, 333-336.

[101] Zhu, C., Jiang, J., Robb, D. A., and Ewins, D. J., 2001, "Active Vibration Control of Rotor System by a Magneto-rheological Fluid Damper," SPIE's 8th Annual International Symposium on Smart Structures and Materials, 4-8-March 2001, Newport Beach, California USA, Conference 4331-13.

[102] Zhu, C., 2001, "Dynamics of a Rotor Supported on Magneto- Rheological Fluid Squeeze Film Damper," *Chinese Journal of Aeronautics*, Vol. 14(1), 6-12.

[103] Kim, K. J., 1999, "Analysis and development of squeeze film damper using Magneto-Rheological fluids," M.Eng. Thesis, Korea Advanced Institute of Science and Technology.

[104] K. J. Kim, J. H. Kim, C. W. Lee, 2000, "Modeling of Magneto-rheological Fluid Based Squeeze Film Damper with Frequency-dependent Parameters," KSME Dynamics and Control Division Summer Conference, Muju.

[105] Suciu, C. V., Bonneau, O., Brun-Picard, D., Frêne, J., and Pascovici, M. D., 2000, "Study of a Novel Squeeze Film Damper and Vibration Generator, *ASME J. Tribology*, Vol. 122, 211-218.